AD-A052 868 CINCINNATI UNIV OH DEPT OF ENGINEERING SCIENCE F/G 12/1
MULTI-RIGID-BODY SYSTEM DYNAMICS WITH APPLICATIONS TO HUMAN-BOD--ETC(U)
AUG 77 R L HUSTON, C E PASSERELLO N00014-75-C-1164
UNCLASSIFIED UC-ES-080177-4-ONR NL

END
DATE FILMED
5-78
DDC

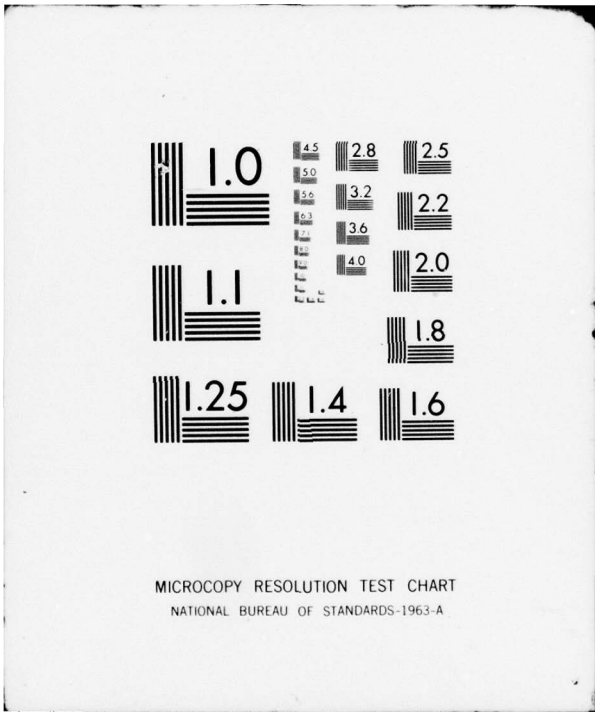
1.0
1.1
1.25
1.4
1.6
1.8
2.0
2.2
2.5
2.8
3.2
3.6
4.0
4.5
5.0
5.6
6.3
MICROCOPY RESOLUTION TEST CHART
NATIONAL BUREAU OF STANDARDS-1963-A

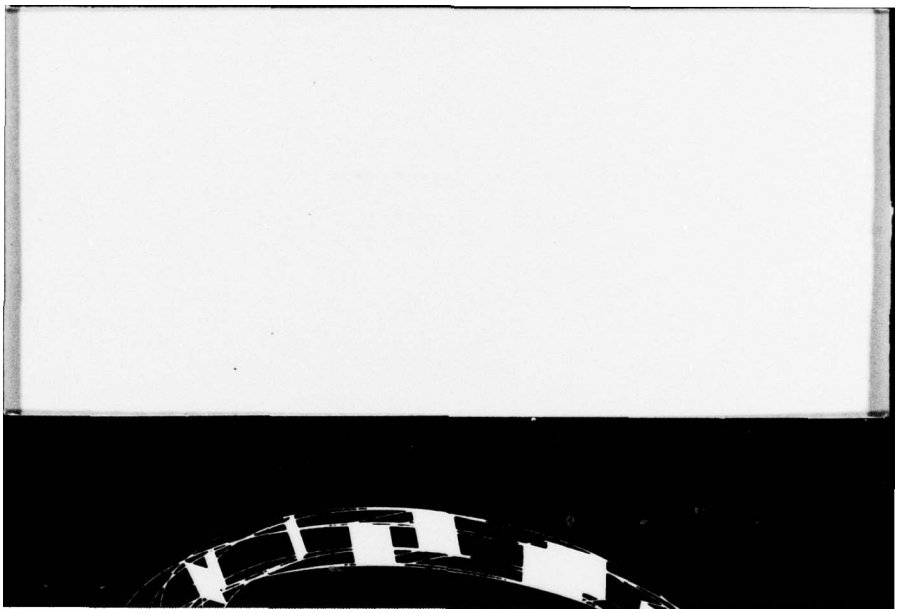

(1)

MULTI-RIGID-BODY SYSTEM DYNAMICS WITH APPLICATIONS TO HUMAN-BODY MODELS AND FINITE-SEGMENT CABLE MODELS

Ronald L. Huston
and
Chris E. Passerello

Final Technical Report under ONR Contract
No. N00014-75-C-1164, NR 064-549 (474)

1 AUG. 1977

ABSTRACT

A computer-oriented method for obtaining dynamical equations of motion for large mechanical systems or "chain systems" is presented. A chain system is defined as an arbitrarily assembled set of rigid bodies such that adjoining bodies have at least one common point and such that closed loops are not formed. The equations of motion are developed through the use of Lagrange's form of d'Alembert's principle.

The method is illustrated and applied with human-body models and finite-segment cable models. The human-body models are configured to simulate a crash-victim. Results with several applied deceleration profiles agree very well with available experimental data. The cable model is configured to simulate an off-shore oil rig or ship's crane with a partially submerged towing cable.

CONTENTS

I.	INTRODUCTION	1
II.	PRELIMINARY CONSIDERATIONS	5
	Body Connection Array	5
	Shifter Transformation Matrices	7
	Shifter Derivatives	9
III.	KINEMATICS	11
	Degrees of Freedom and Generalized Coordinates	11
	Angular Velocities	11
	Angular Accelerations	14
	Mass Center Velocities	16
	Mass Center Accelerations	17
IV.	EQUATIONS OF MOTION	18
	Kinetics	19
	Governing Equations	20
V.	APPLICATION WITH HUMAN-BODY MODELS	22
	The UCIN Model	23
	The UCIN-CRASH Computer Code: Input/Output	29
	Validation of the Model and Examples	32
VI.	APPLICATION WITH FINITE-SEGMENT CABLE MODELS	40
	Equations of Motion, Computer Code, and Numerical Solutions	41
	Example Application	46
VII.	DISCUSSION AND CONCLUSIONS	51
	REFERENCES	53

I. INTRODUCTION

Many mechanical systems and devices can be effectively modelled by systems of rigid bodies. If a rigid-body model of a mechanical system (called a "finite-segment" model) consists of a system of connected (that is, non-disjoint) linked rigid bodies which do not form closed loops or circuits, it is called a "general chain system" (or "open-chain") Figure 1. depicts such a system. The bodies are "linked" such that adjacent bodies share at least one common point, thus allowing for either hinge or ball-and-socket connections. Examples of general chain systems are: human-body models; chain and finite-segment cable models; manipulators; and finite-segment antenna and beam models.

Recently there have been a number of attempts to develop efficient methods for obtaining equations of motion for such systems [1-13]*. These efforts generally proceed by first modelling or replacing the given dynamical system by a discrete system or chain of interconnected rigid bodies. Dynamical equations of motion are then written for the chain system. In the derivation of these equations, some investigators use Lagrange's equations, some use Newton's laws, and some use other modified geometrical theories. But each has the objective of efficient derivation of computer-oriented equations. The relative advantages and disadvantages of these various methods depends upon:

---

*Numbers in brackets refer to references at the end of the Report.

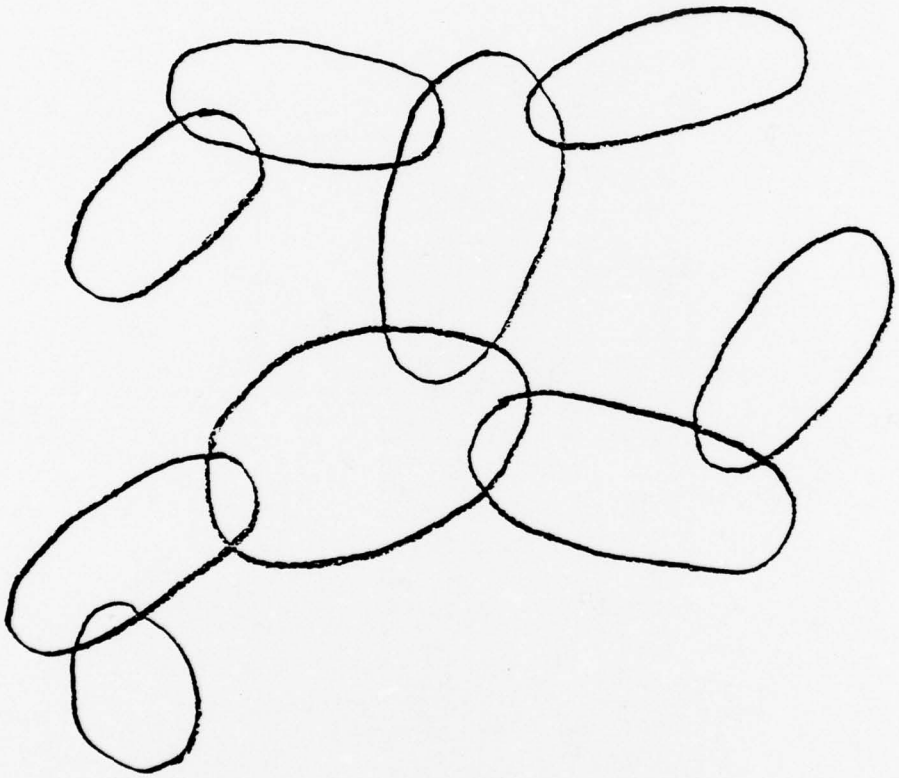

Figure 1. A General Chain System

(i) the particular dynamical principle which is used, and (ii) the method of organizing the complex geometry. The difficulties encountered in these approaches usually include some, and sometimes all, of the following: (i) the introduction of non-working constraint forces between adjoining bodies (eq. Newton's laws); (ii) the tedious, often unwieldy, calculation of derivatives (eq. Lagrange's equations); (iii) the complex geometrical description of the system; and (iv) the solution of the developed equations.

In this report a method of obtaining equations of motion is presented which systematically avoids each of these difficulties. The method uses Lagrange's form of d'Alembert's principle [14-17] which provides for the automatic elimination of the non-working internal constraint forces without introducing tedious differentiation or other calculation. The method also uses a geometrical organization and accounting procedure as developed by Kane [16] and Huston and Passerello [8,10,12,18,19]. The method allows the system to be in any general force field and either the moments or the orientation between adjoining bodies may be specified or left unknown. Finally, the method leads to governing equations which may easily be applied with any general chain system such as human-body models, finite-segment cable models, manipulor models or flexible beam models. Furthermore, the form of the governing equations is ideally suited for developing computer algorithms for obtaining numerical solutions.

The report basically outlines the results of research under the support of the Office of Naval Research Contract N00014-75-C-1164. It contains results of the application of the above method with human-body

models in high-acceleration environments (crashes) and with partially submerged towing cables.

The balance of the report is devided into six parts with the following part presenting some geometrical background, notation, and other preliminary ideas useful in the analysis. The kinematics, dynamics, and governing equations are developed in the next two parts. The application with human-body models and cable models are presented in the subsequent two parts, and a brief discussion and set of conclusions are presented in the final part.

II. PRELIMINARY CONSIDERATIONS

Body Connection Array

Consider the chain system shown in Figure 1. To organize the geometrical accounting of this system, select one body of the system as the reference body and call it B_1. Next, number or label the other bodies of the system in ascending progression away from B_1 as shown in Figure 2. The configuration and kinematics of each body of the system may now be developed relative to B_1 which in turn has its configuration defined relative to an inertial reference frame R (Figure 2.)*.

Although this numbering scheme does not lead to a unique labelling of the bodies, it can nevertheless be used to describe the chain structure through the "body connection array" as follows: Let L(k), k=1, ..., N be an array listing the indices of the adjoining lower-numbered body for each body B_k. For example for the system shown in Figure 2., L(k) is

$$L(k) = (0,1,2,2,4,1,6,1,8) \tag{2.1}$$

where

$$(k) = (1,2,3,4,5,6,7,8,9) \tag{2.2}$$

and where 0 refers to the inertial reference frame R. It is not difficult to see that given L(k) one could readily define the topology or arrangement of the system. That is, Figure 2. could be constructed by simply knowing L(k). It is shown in Part III of the report that L(k)

---

*An alternative approach is to reference each body independently to R, but this is found to be very inconvenient in describing the configuration of actual systems.

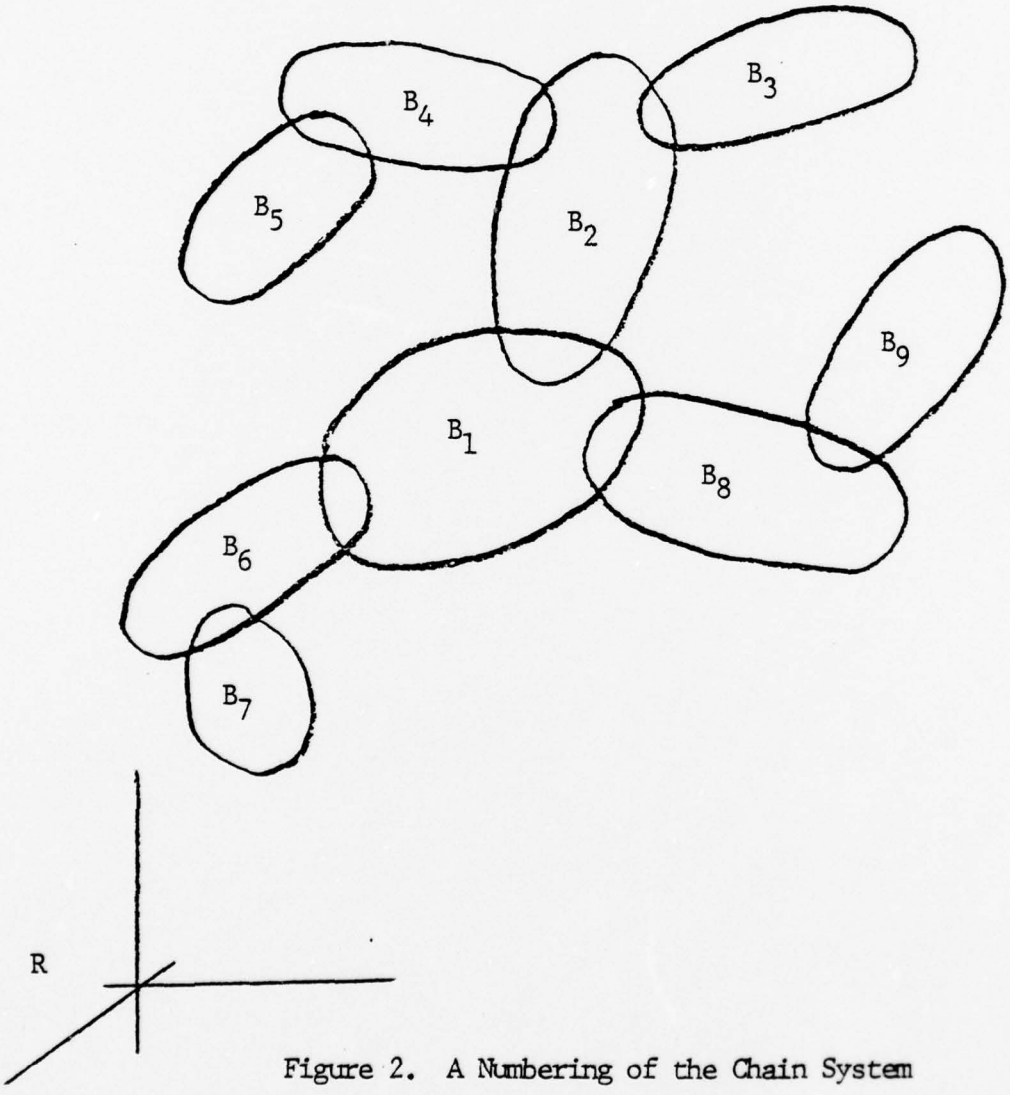

Figure 2. A Numbering of the Chain System

can be useful in the development of expressions of kinematical quantities needed for an analysis of the system's dynamics.

Shifter Transformation Matrices

Next, consider a typical pair of adjoining bodies such as B_j and B_k as shown in Figure 3. The orientation of B_k relative to B_j may be defined in terms of the relative inclinations of the dextral orthogonal unit vector sets, $\underset{\sim}{n}_{ji}$ and $\underset{\sim}{n}_{ki}$ (i=1,2,3) fixed in B_j and B_k as shown in Figure 3. Specifically, let B_j and B_k be oriented such that the $\underset{\sim}{n}_{ji}$ and the $\underset{\sim}{n}_{ki}$ are respectively parallel. Then B_k may be brought into any orientation relative to B_j by three successive dextral rotations about axes parallel to $\underset{\sim}{n}_{k1}$, $\underset{\sim}{n}_{k2}$, and $\underset{\sim}{n}_{k3}$ through the angles α_k, β_k, and γ_k. $\underset{\sim}{n}_{ji}$ and $\underset{\sim}{n}_{ki}$ are then related to each other as

$$\underset{\sim}{n}_{ji} = SJK_{im}\, \underset{\sim}{n}_{km} \tag{2.3}$$

where SJK is a 3 × 3 orthogonal transformation matrix called a "shifter" and defined as [20,21,22]:

$$SJK_{im} = \underset{\sim}{n}_{ji} \cdot \underset{\sim}{n}_{km} \tag{2.4}$$

(Regarding notation, repeated indices, such as m in the right side of Equation (2.3) represent a sum over the range (eg. 1, ...,3) of that index.)

SJK may itself be written as the product of three orthogonal transformation matrices as [19]:

$$SJK = \alpha JK\ \beta JK\ \gamma JK \tag{2.5}$$

where αJK, βJK, and γJK are

$$\alpha JK = \begin{vmatrix} 1 & 0 & 0 \\ 0 & C\alpha_k & -S\alpha_k \\ 0 & S\alpha_k & C\alpha k \end{vmatrix}$$

$$\beta JK = \begin{vmatrix} C\beta_k & 0 & S\beta_k \\ 0 & 1 & 0 \\ -S\beta_k & 0 & C\beta_k \end{vmatrix} \qquad (2.6)$$

$$\gamma JK = \begin{vmatrix} C\gamma_k & -S\gamma_k & 0 \\ S\gamma_k & C\gamma_k & 0 \\ 0 & 0 & 1 \end{vmatrix}$$

where S and C are abbreviations for sine and cosine respectively.

From Equation (2.3) it can be seen that the shifter transformation matrix obeys the following identity rules:

$$SJJ = I = SJK\ SKJ = SJK\ SJK^{-1} \qquad (2.7)$$

where I is the identity matrix. Also, with <u>three</u> bodies, say B_j, B_k, and B_ℓ, the shifter obeys the chain rule:

$$SJL = SJK\ SKL \qquad (2.8)$$

These expressions may be used to transfer components of vectors referred unit vectors in one body of the system into components of vectors referred to unit vectors in any other body of the system and, in particular, to the inertial reference frame R. For example, if a

typical vector $\underset{\sim}{v}$ is expressed as

$$\underset{\sim}{v} = v_i^{(k)} \underset{\sim}{\eta}_{ki} = v_i^{(o)} \underset{\sim}{\eta}_{oi} \tag{2.9}$$

then

$$v_i^{(o)} = SOK_{ij} \, v_j^{(k)} \tag{2.10}$$

where the index o refers to the inertial reference frame R. (There is no sum over repeated indices in parentheses.)

Shifter Derivatives

Finally, since the shifter transformation matrices play a central role throughout the analysis, it is helpful to also have algorithms for their derivatives, especially the derivative of SOK. Such an algorithm may be obtained through Equation (2.4). For SOK, Equation (2.4) may be written in the form:

$$SOK_{ij} = \underset{\sim}{\eta}_{oi} \cdot \underset{\sim}{\eta}_{kj} \tag{2.11}$$

where the η_{oi} are fixed, and therefore constant, in R. Hence, differentiating in Equation (2.11) leads to

$$d(SOK_{ij})/dt = \underset{\sim}{\eta}_{oi} \cdot {}^{R}d\,\underset{\sim}{\eta}_{kj}\,/dt \tag{2.12}$$

where the index R in ${}^{R}d\,\underset{\sim}{\eta}_{kj}\,/dt$ indicates that the derivative of $\underset{\sim}{\eta}_{kj}$ is computed in R. (See Reference [23].) However, since the $\underset{\sim}{\eta}_{kj}$ are fixed in B_k, their derivatives may be written as $\underset{\sim}{\omega}_k \times \underset{\sim}{\eta}_{kj}$ where $\underset{\sim}{\omega}_k$ is the angular velocity of B_k in R [23]. Equation (2.12) may then be written as

$$\begin{aligned} d(SOK_{ij})/dt &= \underset{\sim}{\eta}_{oi} \cdot \underset{\sim}{\omega}_k \times \underset{\sim}{\eta}_{kj} = -\underset{\sim}{\omega}_k \times \underset{\sim}{\eta}_{oi} \cdot \underset{\sim}{\eta}_{kj} \\ &= -e_{imn}\, \omega_{kn}\, \underset{\sim}{\eta}_{om} \cdot \underset{\sim}{\eta}_{kj} \end{aligned} \tag{2.13}$$

or as

$$d(SOK)/dt = WOK\ SOK \tag{2.14}$$

where WOK is a matrix defined as

$$SOK_{im} = - e_{imn}\ \omega_{kn} \tag{2.15}$$

and where ω_{kn} are the components of $\underset{\sim}{\omega}_k$ referred to $\underset{\sim}{\eta}_{on}$ and e_{imn} is the standard permutation symbol [20,22]. (WOK is simply the matrix whose dual vector [22] is $\underset{\sim}{\omega}_k$.)

Equation (2.14) shows that the derivative of the shifter matrix may be computed by a matrix multiplication and thus is ideally suited for development into a numerical, computer algorithm.

III. KINEMATICS

Degrees of Freedom and Generalized Coordinates

The chain system shown in Figure 1. will, in general, have $3N + 3$ degrees of freedom. These may be defined in terms of $3N + 3$ generalized coordinates χ_j $(j=1, \ldots, 3N+3)$. Let χ_1, χ_2, and χ_3 represent the position coordinates of an arbitrarily selected reference point say 0_1 of B_1 in R (See Figure 4.). Then let the remaining $3N$ coordinates be divided into N triplets of coordinates representing the relative orientation angles of the adjoining bodies as described above. For example, χ_4, χ_5, and χ_6 define the orientation of B_1 in R and χ_{3k+1}, χ_{3k+2}, and χ_{3k+3} define the orientation of B_k relative to B_j where B_j is the adjacent lower numbered body to a typical body B_k (See Figure 3.)

Angular Velocities

The angular velocity of a typical body of the system, say B_k, relative to R is readily obtained by the familiar addition formula [16,23] as

$$\underset{\sim}{\omega}_k = \hat{\omega}_1 + \ldots \hat{\omega}_k \tag{3.1}$$

where the terms on the right represent angular velocities of the subscripted body relative to its adjacent, lower-numbered body, and where the sum is taken over the bodies in the chain from B_1 outward through the branch containing B_k. For example, referring to Figure 2., $\underset{\sim}{\omega}_5$ is

$$\underset{\sim}{\omega}_5 = \hat{\underset{\sim}{\omega}}_1 + \hat{\underset{\sim}{\omega}}_2 + \hat{\underset{\sim}{\omega}}_4 + \hat{\underset{\sim}{\omega}}_5 \tag{3.2}$$

where $\hat{\omega}_1$ is the angular velocity of B_1 relative to R, $\hat{\omega}_2$ is the angular velocity of B_2 relative to B_1, $\hat{\omega}_4$ is the angular velocity of B_4 relative to B_2, and $\hat{\omega}_5$ is the angular velocity of B_5 relative to B_4. (Regarding notation, the "hats" are used to designate relative angular velocities with respect to the adjacent, lower-numbered body, and the terms without the hats designate absolute angular velocities (that is, relative to R). Hence, ω_1 and $\hat{\omega}_1$ are the same.)

The L(k) array introduced above can be used to form a convenient expression for the sum in Equation (3.1). To see this, consider the example of Equation (3.2). The subscripts on the right side of Equation (3.2) (that is, 1,2,4,5) may be obtained from L(k) as follows: Consider L(k) as a function mapping the (k) array into the L(k) array (See Equations (2.1) and (2.2)). Then, using the notation that $L^0(k) = (k)$, $L^1(k) = L(k)$, $L^2(k) = L(L(k))$, $L^3(k) = L(L^2(k))$, etc., it is seen from Equation (2.1) that

$$L^0(5)=5,\ L^1(5)=4,\ L^2(5)=2,\ L^3(5)=1 \tag{3.3}$$

Therefore, ω_5 may be written as

$$\omega_5 = \sum_{p=0}^{3} \hat{\omega}_q \quad \text{where } q = L^p(5) \tag{3.4}$$

Hence, in general, the angular velocity of B_k may be written as

$$\omega_k = \sum_{p=0}^{r} \hat{\omega}_q \quad \text{where } q = L^p(k) \tag{3.5}$$

and where r is the index such that $L^r(k)=1$.

Now, in view Figure 3., and the description of the relative orientation of B_k with respect to B_j, $\hat{\underset{\sim}{\omega}}_k$ may be written as [19,21]

$$\hat{\underset{\sim}{\omega}}_k = \dot{\alpha}_k \underset{\sim}{N}_{k1} + \dot{\beta}_k \underset{\sim}{N}_{k2} + \dot{\gamma}_k \underset{\sim}{N}_{k3} \quad \text{(no sum on k)} \tag{3.6}$$

where $\underset{\sim}{N}_{k1}$, $\underset{\sim}{N}_{k2}$, and $\underset{\sim}{N}_{k3}$ are unit vectors parallel to $\underset{\sim}{\eta}_{k1}$, $\underset{\sim}{\eta}_{k2}$, and $\underset{\sim}{\eta}_{k3}$ during the successive dextral rotations defining α_k, β_k, and γ_k as described in the foregoing part of the report. In terms of $\underset{\sim}{\eta}_{ji}$ (i=1,2,3), the unit vectors fixed in B_j, the adjacent lower numbered body, $\underset{\sim}{N}_{ki}$ (i=1,2,3) are

$$\begin{aligned} \underset{\sim}{N}_{k1} &= \underset{\sim}{\eta}_{j1} = \delta_{m1} \underset{\sim}{\eta}_{jm} \\ \underset{\sim}{N}_{k2} &= \alpha JK_{m2} \underset{\sim}{\eta}_{jm} \\ \underset{\sim}{N}_{k3} &= \alpha JK_{mp} \beta JK_{p3} \underset{\sim}{\eta}_{jm} \end{aligned} \tag{3.7}$$

Hence, $\hat{\underset{\sim}{\omega}}_k$ becomes

$$\hat{\underset{\sim}{\omega}}_k = (\dot{\alpha}_k \delta_{m1} + \dot{\beta}_k \alpha JK_{m2} + \dot{\gamma}_k \alpha JK_{mp} \beta JK_{p3}) \underset{\sim}{\eta}_{jm} \tag{3.8}$$

or in terms of $\underset{\sim}{\eta}_{oi}$, the unit vectors fixed in R

$$\hat{\underset{\sim}{\omega}}_k = SOJ_{im} (\dot{\alpha}_k \delta_{m1} + \dot{\beta}_k \alpha JK_{m2} + \dot{\gamma}_k \alpha JK_{mp} \beta JK_{p3}) \underset{\sim}{\eta}_{jm} \tag{3.9}$$

By substituting from Equation (3.9) into Equation (3.5), $\underset{\sim}{\omega}_k$ may be written in the form

$$\underset{\sim}{\omega}_k = \omega_{k\ell m} \dot{X}_\ell \underset{\sim}{\eta}_{om} \tag{3.10}$$

where there is a sum from 1 to 3N+3 on ℓ and from 1 to 3 on m. From Equation (3.9), it is seen that the non-zero $\omega_{k\ell m}$ take one of the

three forms

$$\omega_{k\ell m} = \begin{matrix} SOJ_{m1} \\ SOJ_{mn}\alpha JK_{n2} \\ SOJ_{mn}\alpha JK_{np}\beta JK_{p3} \end{matrix} \qquad (3.11)$$

depending on whether χ_ℓ is the first, second, or third dextral angle defining the orientation of B_k relative to B_j. Also, from Equation (3.5) it is seen that for two bodies B_r and B_s, in the same branch of the chain, $\omega_{r\ell m} = \omega_{s\ell m}$ for r greater than s, if $\omega_{s\ell m} \neq 0$.

Angular Accelerations

The angular acceleration of B_k relative to R may be obtained by differentiating the angular velocity expression of Equation (3.10). Noting that the $n_{\sim om}$ are fixed in R, this leads to

$$\alpha_k = (\omega_{k\ell m}\ddot{\chi}_\ell + \dot{\omega}_{k\ell m}\dot{\chi}_\ell)n_{\sim om} \qquad (3.12)$$

From Equation (3.11), the non-zero $\dot{\omega}_{k\ell m}$ are found to take one of the three forms:

$$\dot{\omega}_{k\ell m} = \begin{matrix} S\dot{O}J_{m1} \\ S\dot{O}J_{mn}\alpha JK_{n2} + SOJ_{mn}\,\alpha\dot{J}K_{n2} \\ S\dot{O}J_{mn}\,\alpha JK_{np}\,\beta JK_{p3} + SOJ_{mn}\,\alpha\dot{J}K_{np}\beta JK_{p3} \\ + SOJ_{mn}\,\alpha JK_{np} + \beta\dot{J}K_{p3} \end{matrix} \qquad (3.13)$$

depending on whether χ_ℓ is the first, second, or third dextral angle defining the orientation of B_k relative to B_j. The $S\dot{O}J$ are given by

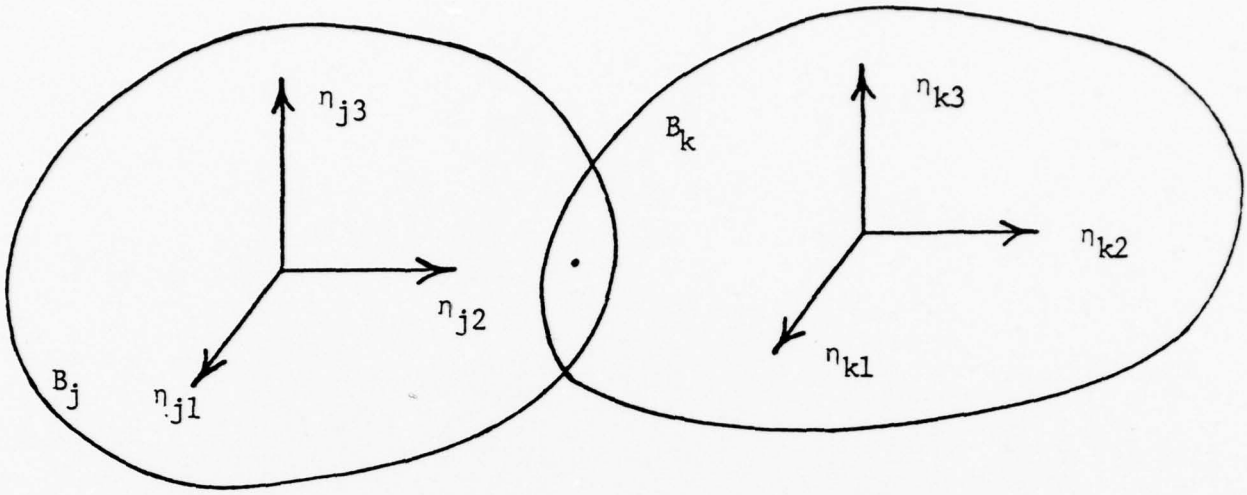

Figure 3. Two Typical Adjoining Bodies

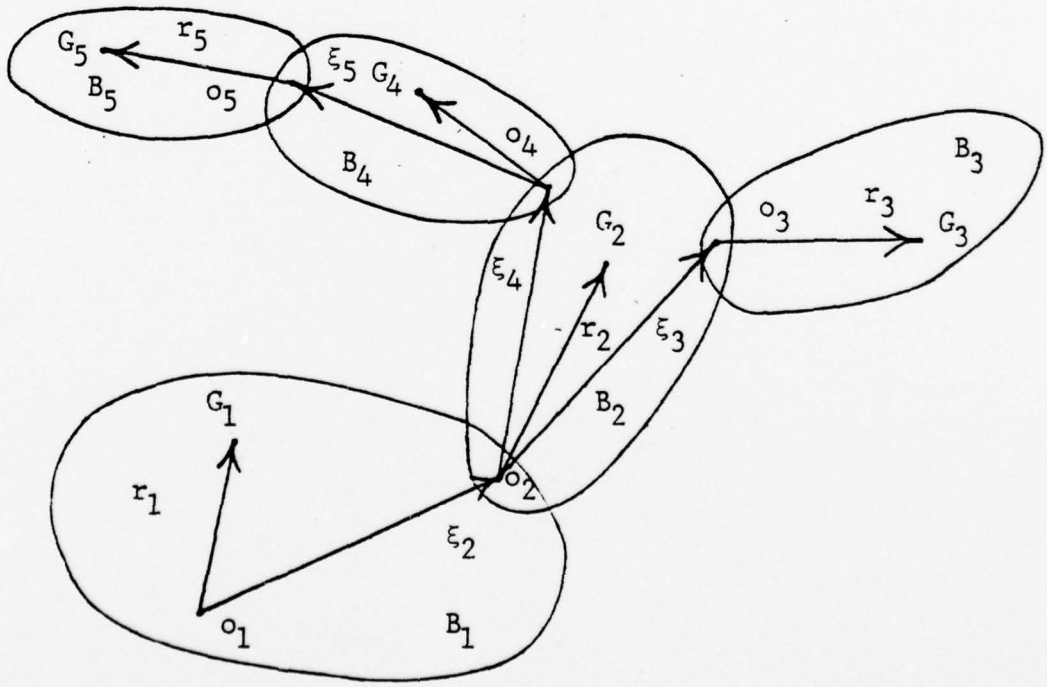

Figure 4. Mass Centers, Reference Points and Locating Position Vectors

Equation (2.14) and the αJK and βJK are obtained by differentiating the expressions in Equation (2.6).

Mass Center Velocities

The velocity and acceleration, relative to R, of the mass centers of the bodies of the system may be obtained as follows: First, recall that O_1 is an arbitrarily selected reference point of B_1 (See Figure 4., for example). Next, let O_k be the connection point or common point of two typical bodies, say B_k and B_j where B_j is the adjacent lower-numbered body of B_k ($k=2, \ldots, N$), and let O_k be called the "reference point" of B_k. Then let $\underset{\sim}{\xi}_k$ be the position vector of O_k relative to O_j. Finally, let G_k be the mass center of B_k ($k=1, \ldots, N$), and let $\underset{\sim}{r}_k$ be the position vector of G_k relative to O_k. ($\underset{\sim}{\xi}_k$ is thus fixed in B_j and $\underset{\sim}{r}_k$ is fixed in B_k.) Hence, the position vector $\underset{\sim}{P}_k$ of G_k relative to a fixed point 0, in R may be written as

$$\underset{\sim}{P}_k = (\xi_{oi} + SOK_{ih}\, \gamma_{kh} + \sum_{q=0}^{u-1} SOS_{ih}\, \xi_{sh})\, \underset{\sim}{n}_{oi} \qquad (3.14)$$

where $s=L^{\beta}(k)$, $S=L^{\beta+1}(k)$, and u is the index such that $L^u(k)=1$, and where $\underset{\sim}{\xi}_o$ is the position vector of O_1 relative to 0. Therefore, by differentiating $\underset{\sim}{P}_k$ in R, the velocity of G_k in R is

$$\underset{\sim}{v}_k = (\dot{\xi}_{oi} + \dot{SOK}_{ih}\, r_{kh} + \sum_{q=0}^{u-1} \dot{SOS}_{ih}\, \xi_{sh})\, \underset{\sim}{n}_{oi} \qquad (3.15)$$

By using Equations (2.14), (2.15), and (3.10), $\underset{\sim}{v}_k$ may be written in the form

$$\underset{\sim}{v}_k = v_{k\ell m}\, \dot{\chi}_\ell\, \underset{\sim}{n}_{om} \qquad (3.16)$$

where the non-zero $v_{k\ell m}$ are

$$v_{k\ell m} = \delta_{\ell m} \quad (k=1,\ldots,N;\ \ell,m=1,2,3) \tag{3.17}$$

and

$$v_{k\ell m} = WK_{mh\ell}\, r_{kh} + \sum_{q=0}^{u-1} WS_{mh\ell}\, \xi_{sh} \tag{3.18}$$

$$(k=1,\ldots,N;\ \ell=1,\ldots,3N+3;\ m=1,2,3)$$

where $WK_{mh\ell}$ is defined as

$$WK_{mh\ell} = \frac{\partial WOK_{mp}}{\partial \dot{\chi}_\ell} \quad SOK_{ph} = -\, e_{mpq}\, \omega_{k\ell q}\, SOK_{ph} \tag{3.19}$$

Mass Center Accelerations

The acceleration of G_k in R is now obtained by differentiating $\underset{\sim}{v}_k$ in Equation (3.16). This leads to

$$\underset{\sim}{a}_k = (v_{k\ell m}\, \ddot{\chi}_\ell + \dot{v}_{k\ell m}\, \dot{\chi}_\ell)\, \underset{\sim}{n}_m \tag{3.20}$$

where the non-zero $\dot{v}_{k\ell m}$ are

$$\dot{v}_{k\ell m} = \dot{WK}_{mh\ell}\, r_{kh} + \sum_{q=0}^{u-1} \dot{WS}_{mh\ell}\, \xi_{sh} \tag{3.21}$$

where $\dot{WK}_{mh\ell}$ is

$$\dot{WK}_{mh\ell} = -e_{mpq}(\dot{\omega}_{k\ell q}\, SOK_{ph} + \omega_{k\ell q}\, \dot{SOK}_{ph}) \tag{3.22}$$

IV. EQUATIONS OF MOTION

As mentioned earlier, the governing dynamical equations of motion of a general chain system such as is shown in Figure 1., can be obtained conveniently using Lagrange's Form of d'Alembert's principle [14,17]. Since the non-working internal constraint forces acting between the bodies of the system are automatically eliminated in using this principle, only the externally applied, or active forces, acting on the system, and the so-called inertia forces of the system need be considered in the analysis.

Kinetics

Imagine the system of Figure 1. to be subjected to an arbitrary external force field. Then let the ensuing forces acting on a typical body B_k of the system be replaced by an equivalent force system consisting of a single force $\underset{\sim}{F}_k$ passing through G_k together with a couple with torque $\underset{\sim}{M}_k$. Then the so-called "generalized active force" F_ℓ, corresponding to the generalized coordinate χ_ℓ, acting on B_k is [16]

$$F_\ell = v_{k\ell m} F_{km} + {}_k\, {}_m M_{km} \quad (\ell = 1,\ldots,3N+3;\ k=1,\ldots,N) \tag{4.1}$$

where there is no sum on k, but there is a sum from 1 to 3 on m. F_{km} and M_{km} are the $\underset{\sim}{\eta}_{om}$ components of $\underset{\sim}{F}_k$ and $\underset{\sim}{M}_k$ respectively. Now, if the generalized active forces of each of the bodies of the system are added together, the result is the total generalized active force for the entire system. Hence, if there is a sum over k from 1 to N

in Equation (4.1), then F_ℓ represents the total generalized active force on the system for the generalized coordinate χ_ℓ (ℓ=1,...,3N+3).

In a similar manner, let the inertia forces on a typical body B_k of the system be replaced by a single force $\underset{\sim}{F}^*_k$ passing through G_k together with a couple with torque $\underset{\sim}{M}^*_k$. Then $\underset{\sim}{F}^*_k$ and $\underset{\sim}{M}^*_k$ may be written as [16]:

$$\underset{\sim}{F}^*_k = -m_k \underset{\sim}{a}_k \quad \text{(no sum)} \tag{4.2}$$

and

$$\underset{\sim}{M}^*_k = -\underset{\sim}{I}_k \cdot \underset{\sim}{\alpha}_k - \underset{\sim}{\omega}_k \times (\underset{\sim}{I}_k \cdot \underset{\sim}{\omega}_k) \tag{4.3}$$

where m_k is the mass of B_k and $\underset{\sim}{I}_k$ is the inertia dyadic of B_k relative to G_k (k=1,..., N). Through use of the shifter transformation matrices $\underset{\sim}{I}_k$ may be written in the form

$$\underset{\sim}{I}_k = I_{kmn}\, \underset{\sim}{\eta}_{Om}\, \underset{\sim}{\eta}_{On} \tag{4.4}$$

The so-called "generalized inertia force" F_ℓ^*, corresponding to the generalized coordinate χ_ℓ, acting on B_k is then [16]

$$F_\ell^* = v_{k\ell m}\, F^*_{km} + \omega_{k\ell m}\, M^*_{km} \quad (\ell=1,\ldots,3N+3;\ k=1,\ldots,N) \tag{4.5}$$

where there is no sum on k, there is a sum from 1 to 3 on m, and F^*_{km} and M^*_{km} are the $\underset{\sim}{\eta}_{Om}$ components of $\underset{\sim}{F}^*_k$ and $\underset{\sim}{M}^*_k$ respectively. As above, if the generalized inertia forces of each of the bodies of the system are added together, the result is the total generalized inertia force for the entire system. Hence, if there is a sum over k from 1 to N in Equation (4.2), then F_ℓ^* represents the total generalized

inertia force on the system for the generalized coordinate χ_ℓ (ℓ=1,...,3N+3).

Governing Equations

Lagrange's form of d'Alembert's principle states that the sum of the total generalized active force and the total generalized inertia force, for each generalized coordinate of the system, is zero. Hence, the governing dynamical equations of motion for the system are

$$F_\ell + F_\ell^* = 0 \quad (\ell=1,\ldots,3N+3) \tag{4.6}$$

By substituting Equations (3.10), (3.12), and (3.20) into Equations (4.2) and (4.3) and ultimately into Equations (4.6), the governing equations of motion may be written in the form

$$a_{\ell p}\, \ddot{\chi}_p = f_\ell \quad (\ell=1,\ldots,3N+3) \tag{4.7}$$

where there is a sum from 1 to 3N+3 on p and where $a_{\ell p}$ and f_ℓ are given by

$$a_{\ell p} = m_k v_{kpm} v_{k\ell m} + I_{kmn}\, \omega_{kpm}\, \omega_{k\ell n} \tag{4.8}$$

and

$$f_\ell = -(F_\ell + m_k\, v_{k\ell m}\, v_{kqm}\, \dot{\chi}_q + I_{kmn}\, \omega_{k\ell m}\, \dot{\omega}_{kqn}\, \dot{\chi}_q + e_{rmh}\, I_{kmr}\, \omega_{kqn}\, \omega_{ksr}\, \omega_{k\ell h}\, \dot{\chi}_q\, \dot{\chi}_s) \tag{4.9}$$

where there is a sum from 1 to N on k, from 1 to 3N+3 on q and s, and from 1 to 3 on the other repeated indices.

Equations (4.7) form a set of 3N+3 simultaneous ordinary differential equations for the 3N+3 generalized coordinates χ_ℓ of the system. If some (or all) of the χ_ℓ are specified, the differential equations become algebraic equations for the unknown forces or moments

associated with the specified χ_ℓ. Since the coefficients, $a_{\ell p}$ and f_ℓ, of these equations are simple polynomial functions of the physical parameters and the four block matrices $\omega_{k\ell m}$, $\dot{\omega}_{k\ell m}$, $v_{k\ell m}$, and $\dot{v}_{k\ell m}$, computer algorithms may easily be written for the numerical development of the equations. Moreover, once they are developed they may also be solved numerically using one of the standard numerical integration routines.

In the following two parts of the report these equations are developed and solved for a human-body model in a variety of high-acceleration configurations, and for a finite-segment cable model.

V. APPLICATION WITH HUMAN-BODY MODELS

As mentioned earlier, a principal application of the foregoing analysis is studying the dynamics of a human-body model. Indeed, a desire to obtain insight into the dynamics of space-walking astronauts, athletes, and crash-victims has stimulated much of the development of the foregoing analysis.

Gross motion simulation of the human body naturally leads to finite-segment or chain-system modelling if one thinks of the human body in terms of its skeletal structure. That is, by considering the hands, feet, arms, legs, head, and torso as rigid bodies and the muscles and ligaments as springs and dampers acting at the joints, the ensuing model is precisely a general chain system as studied in the foregoing parts of the report. In this part of the report a summary of research results obtained by using the analysis in the development and application of a crash-victim computer simulation code [24-29], commonly known as "UCIN", is presented.

There have, of course, been numerous earlier attempts to model the dynamics of the human body and in particular, the dynamics of a crash victim. The number of these efforts significantly increased during the past decade with the availability of high-speed digital computers. Indeed, there even exists a number of recent survey papers [30-33] outlining this work. From these papers it appears that much of the significant work in general human body dynamics and modelling may be found in References [18,19,34-38] and in gross-motion,

crash-victim simulation in References [24-33,39-78]. The specific approaches discussed in References [18,19,24,29] have led to the development of the foregoing general analysis and ultimately to the development of the UCIN model as described in the following section.

The UCIN Model

The model consists of 12 rigid bodies representing the human limbs together with a vehicle cockpit as shown in Figure 5. The twelve bodies of the model are connected together with ball-and-socket joints which allow for the inclusion of springs and dampers to simulate the human connective soft tissue such as discs, muscles, and ligaments.

Forty-five variables are required to describe the position and orientation of the model. These are:

x_1, x_2, x_3	position of the vehicle relative to an inertial frame
x_4, x_5, x_6	orientation of the vehicle relative to an inertial frame
x_7, x_8, x_9	position of a reference point in B_2, the lower torso relative to the origin of the vehicle frame
x_{10}, x_{11}, x_{12}	orientation of B_2, the lower torso, relative to the vehicle frame
x_{13}, x_{14}, x_{15}	orientation of B_3, the middle torso, relative to B_2, the lower torso
x_{16}, x_{17}, x_{18}	orientation of B_4, the upper torso, relative to B_3, the middle torso
x_{19}, x_{20}, x_{21}	orientation of B_5, the upper left arm, relative to B_4, the upper torso
x_{22}, x_{23}, x_{24}	orientation of B_6, the lower left arm relative to B_5, the upper left arm

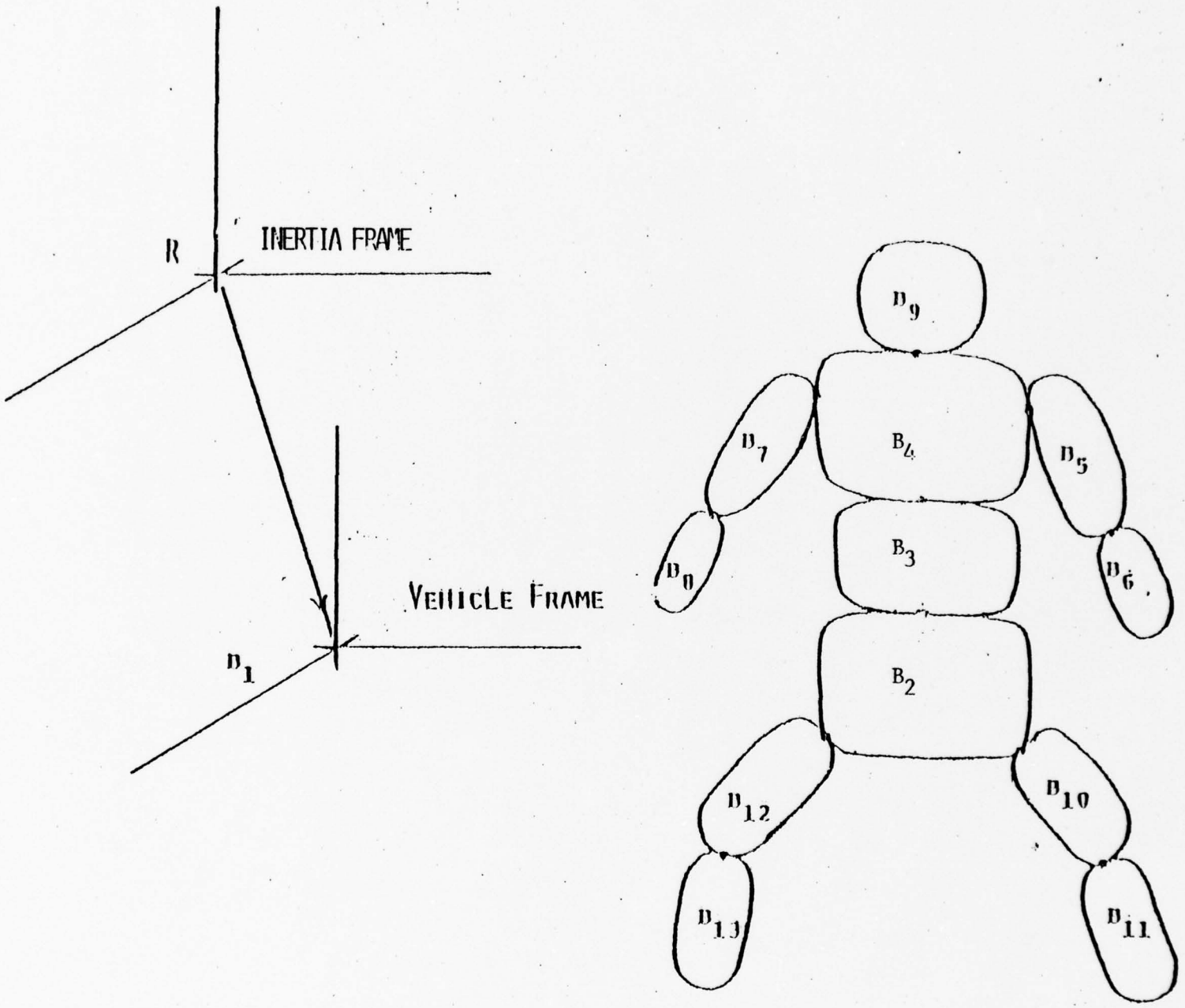

Figure 5. The UCIN Model and Vehicle Cockpit

$\chi_{25}, \chi_{26}, \chi_{27}$	orientation of B_7, the upper right arm, relative to B_4, the upper torso
$\chi_{28}, \chi_{29}, \chi_{30}$	orientation of B_8, the lower right arm, relative to B_7, the upper right arm
$\chi_{31}, \chi_{32}, \chi_{33}$	orientation of B_9, the head relative to B_4, the upper torso
$\chi_{34}, \chi_{35}, \chi_{36}$	orientation of B_{10}, the upper left leg, relative to B_2, the lower torso
$\chi_{37}, \chi_{38}, \chi_{39}$	orientation of B_{11}, the lower left leg, relative to B_{10}, the upper left leg
$\chi_{40}, \chi_{41}, \chi_{42}$	orientation of B_{12}, the upper right leg, relative to B_2, the lower torso
$\chi_{43}, \chi_{44}, \chi_{45}$	orientation of B_{13}, the lower right leg, relative to B_{12}, the upper right leg

All of these variables, except for the position variables χ_1, χ_2, χ_3, χ_7, χ_8, and χ_9 are orientation angles generated by successive rotation of adjacent bodies relative to each other as described in Part II of the Report. The first six variables define the motion of the cockpit or vehicle frame, B_1, relative to the inertial frame, R. These variables must be specified or given. Also, variables χ_{22}, χ_{24}, χ_{28}, χ_{30}, χ_{37}, χ_{39}, χ_{43}, and χ_{45} are usually specified as zero to simulate hinge joints at the elbows and knees. The remaining 31 variables may be either specified or left as unknowns. If the variables are specified (e.g. $\chi_{16}=0$), the required moment needed to maintain that specification (e.g. M_{16}) is determined.

The model accepts arbitrary specification of external forces and moments on each of its bodies. These forces and moments are represented on each body by an equivalent force system consisting of a single force passing through the mass center of the body, together

with a couple.

The model's initial position is generally in an erect sitting position as shown in Figures 6. and 7. In this configuration, all the body coordinate axes and the vehicle frame are aligned. Thus in this configuration, all the orientation angles are zero.

The model has a seat which is modelled by springs as shown in Figure 9. There are seven "one-way" springs which may exert forces on the model with the points of contact being the mass centers of bodies 2, 3, 4, 9, 10, and 12. ("One-way" springs exert forces only while in compression.) One-way viscous damper stops are used to limit the seat deflection. The force F generated by a damper stop is of the form

$$F = \begin{matrix} k\dot{\chi} & \text{if} & \chi > \chi_o \\ 0 & \text{if} & \chi \leq \chi_o \end{matrix} \qquad (5.1)$$

where k is an arbitrary constant, χ is the spring deformation (compression), and χ_o is an arbitrary spring compression limit.

The model has a floor or foot rest which is modelled as a linear spring.

The model provides for the use of up to ten restraining belts modelled as springs attached at arbitrary points between the cockpit and the bodies of the model.

The ball-and-socket connection joints of the model are provided with angle stops, modelled by one-way dampers, to simulate motion constraints of the human limbs. An angle stop generates a moment $\underset{\sim}{M}$ between the bodies of the form

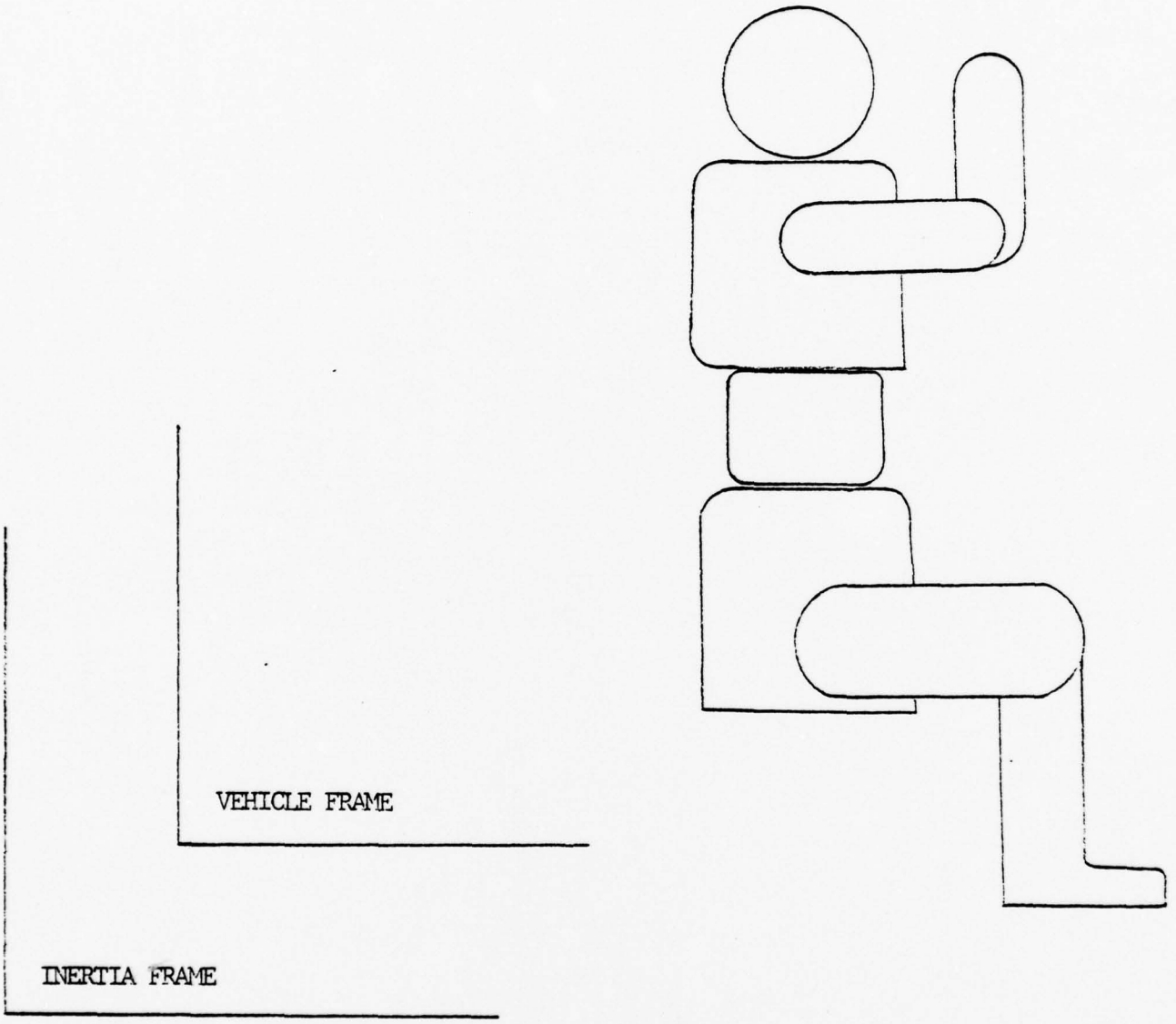

Figure 6. Side View of the Model is a Sitting Configuration

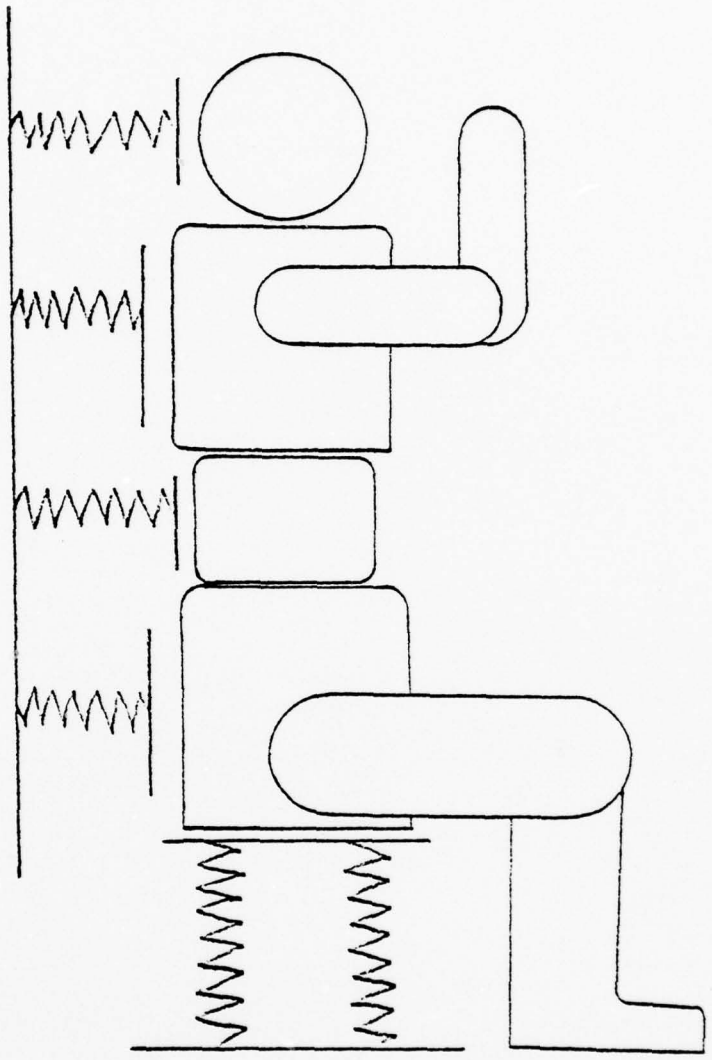

Figure 7. The Model and Seat in Initial Configuration

$$M = \begin{cases} C_0 - C_1(\alpha-\alpha_1)\dot{\alpha} & \text{if} \quad \alpha > \alpha_1 \\ C_0 & \text{if} \quad -\alpha_2 < \alpha < \alpha_1 \\ C_0 + C_1(\alpha-\alpha_2) & \text{if} \quad \alpha < \alpha_2 \end{cases} \tag{5.2}$$

where α is a rotation angle, α_1 and α_2 are arbitrarily specified maximum and minimum values of α, and C_0 and C_1 are arbitrarily specified constants.

Finally, the model provides for the use of twelve intrusion surfaces or planes to simulate the cockpit or vehicle interior. These intrusion surfaces are as follows:

1) Left windshield
2) Front windshield
3) Right windshield
4) Upper left door
5) Lower left door
6) Upper right door
7) Lower right door
8) Roof
9) Firewall
10) Top dash
11) Front dash
12) Bottom dash

The location and inclination of these intrusion surfaces are determined by the specification of the position of a point in the surface together with the components of a vector normal to the surface.

The UCIN-CRASH Computer Code: Input/Output

The following brief paragraphs provide a general description of the input data required and the output data provided by the computer code. Additional details may be obtained from References [27] and [28].

The input consists of the following:

Physical parameters: These are the masses, inertia dyadics, mass center positions, connection point positions, and orientation angle limits, for each of the 12 bodies of the model.

Cockpit geometry: This consists of a normal vector and a location point for each of the 12 intrusion surface planes listed above. Also, the floor position and a spring constant of the floor model are part of the cockpit specifications.

Cockpit motion: The cockpit displacement and rotation relative to an inertia frame $(\chi_1,\ldots,\chi_6)$ are required as input. Typically, it is useful to express this in terms of the linear and angular acceleration of the cockpit. The computer program is written so that the cockpit acceleration components may be "read in" by simply specifying the acceleration profile. (This is, in effect, a piecewise-linear approximation to an acceleration curve.) Six (three translation and three rotation) acceleration profiles or curves may be employed.

Spring and damping constants: These include seat constants, restraining belt constants, orientation angle constants, and neck parameters. Also, the attach points of the restraining belts are included as part of this data.

Initial conditions: This includes the initial values of the unknown variables and their derivatives. Also, the external forces and moments (if any) which are applied to the bodies of the models must be specified.

Integration parameters: This consists of constants required by the fourth-order, Runge-Kutta integration technique (RKGS) and it includes the starting time, the ending time, the step size, and the error permitted.

The output consists of two parts: The first is simply a copy or "echo" of the input data. The second contains at each output step the following:

1) The value of all variables and their first and second derivatives.
2) The joint and mass center positions in both inertia space and relative to the cockpit.
3) The mass center velocities and accelerations.
4) The moments and forces associated with variables which are specified.
5) Restraining belt forces.
6) Collisions or "hits" with intrusion surfaces.

Validation of the Model and Examples

There is little experimental data available to date which can be used to check or verify the above computer code and others like it. However, King, Padgaonkar, and Mital [79] have recently conducted a series of experiments with a cadaver in an impact seat for the purpose of validating the computer model. The results show remarkable agreement between the model and the experiment as shown in Reference [79].

In earlier tests, Begeman, King, and Prasad [80] placed a cadaver in an impact sled and they measured shoulder belt, vertical lap belt and seat pan forces. This same test was simulated with the UCIN computer model. For the deceleration profile shown in Figure 8., the experimental and computed shoulder belt, vertical lap belt, and seat pan forces are shown in Figures 9., 10., and 11.

In another configuration, experimental data from a vehicle striking a guard rail or roadside barrier [81] was used as input for the computer code. For the specific deceleration profile shown in Figure 12., the resultant relative displacement of the head and chest using both lap belts and a combination of both lap and shoulder felts, is shown in Figure 13.

Finally, in an attempt to measure the relative effectiveness of lap and shoulder belts, a run was made simulating a front end collision of a vehicle. The head pitch (forward rotation) of the model was calculated using a lap belt and a combination lap and shoulder belt. The results shown in Figure 14. illustrate the "whiplash" effect when only lap belts are used.

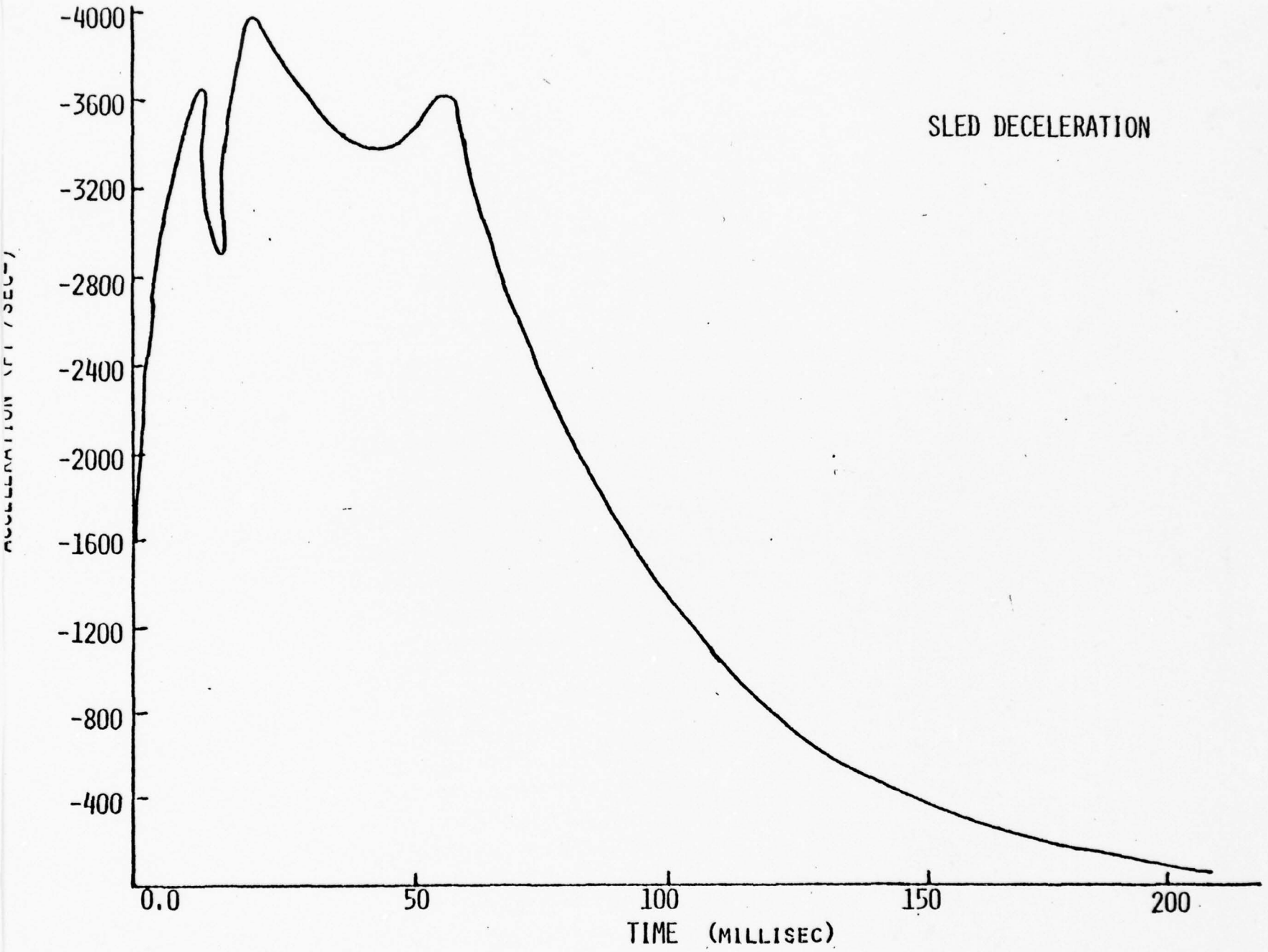

Figure 8. Impact Sled Deceleration

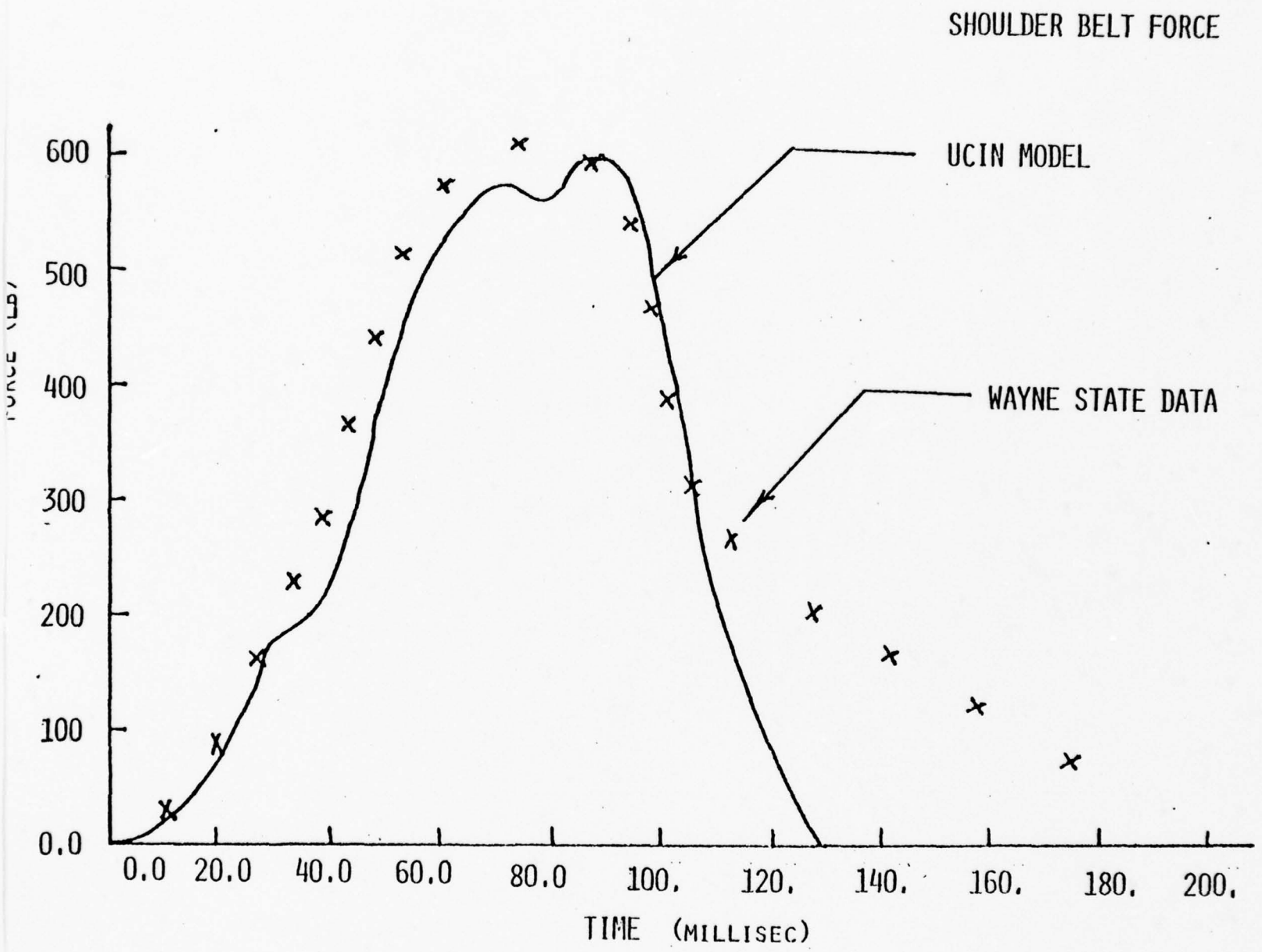

Figure 9. Comparison of Shoulder Belt Forces

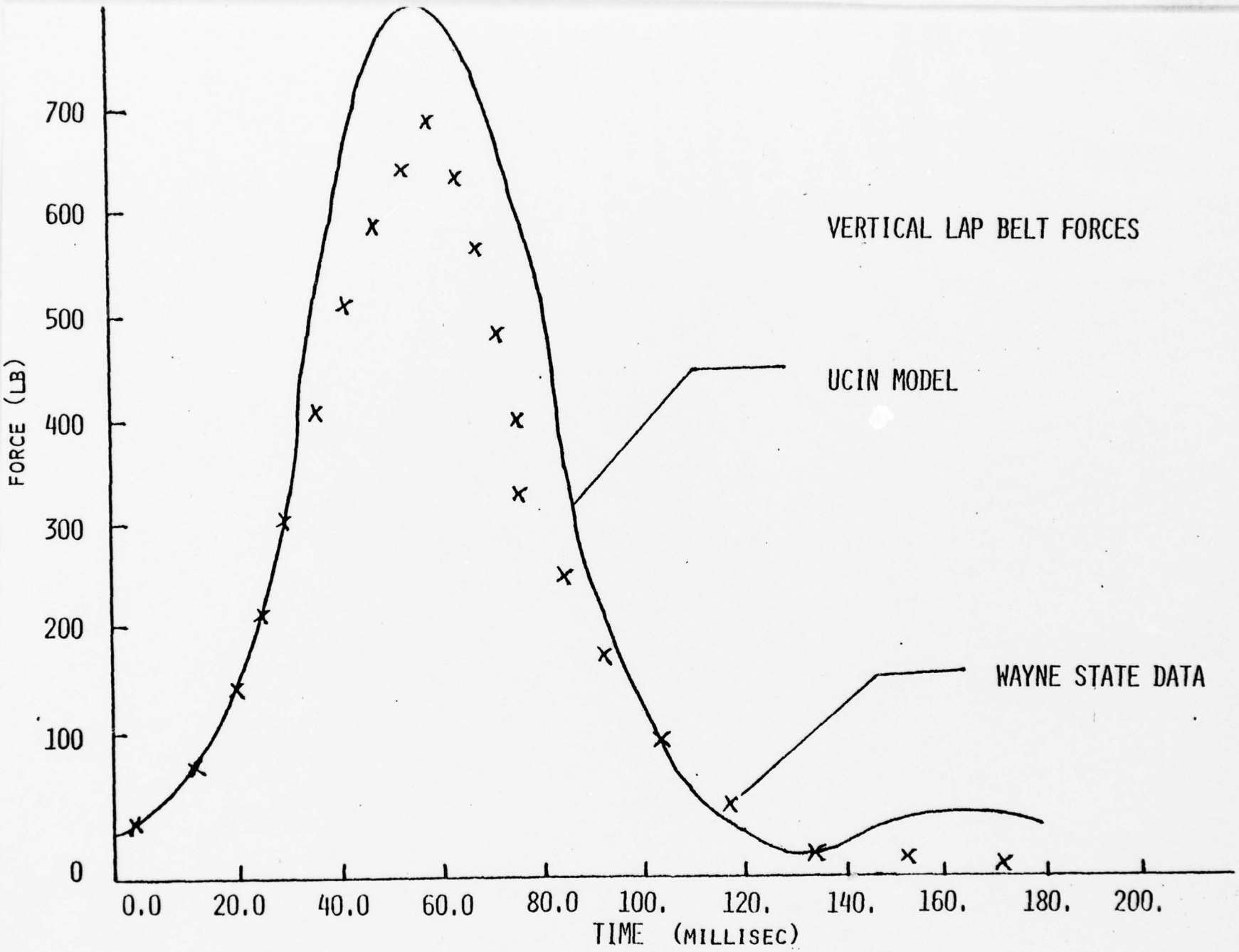

Figure 10. Comparison of Vertical Lap Belt Forces

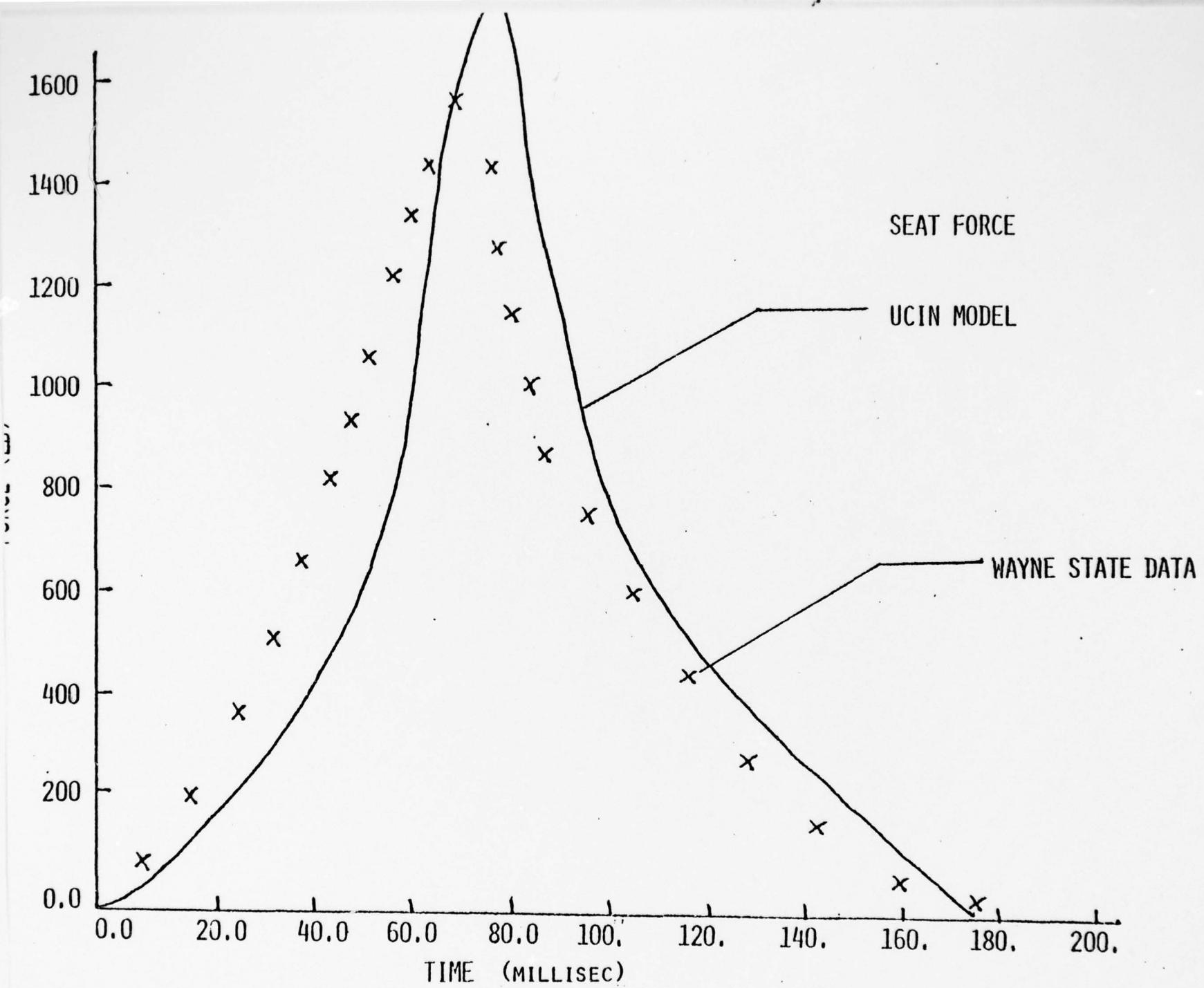

Figure 11. Comparison of Seat Forces

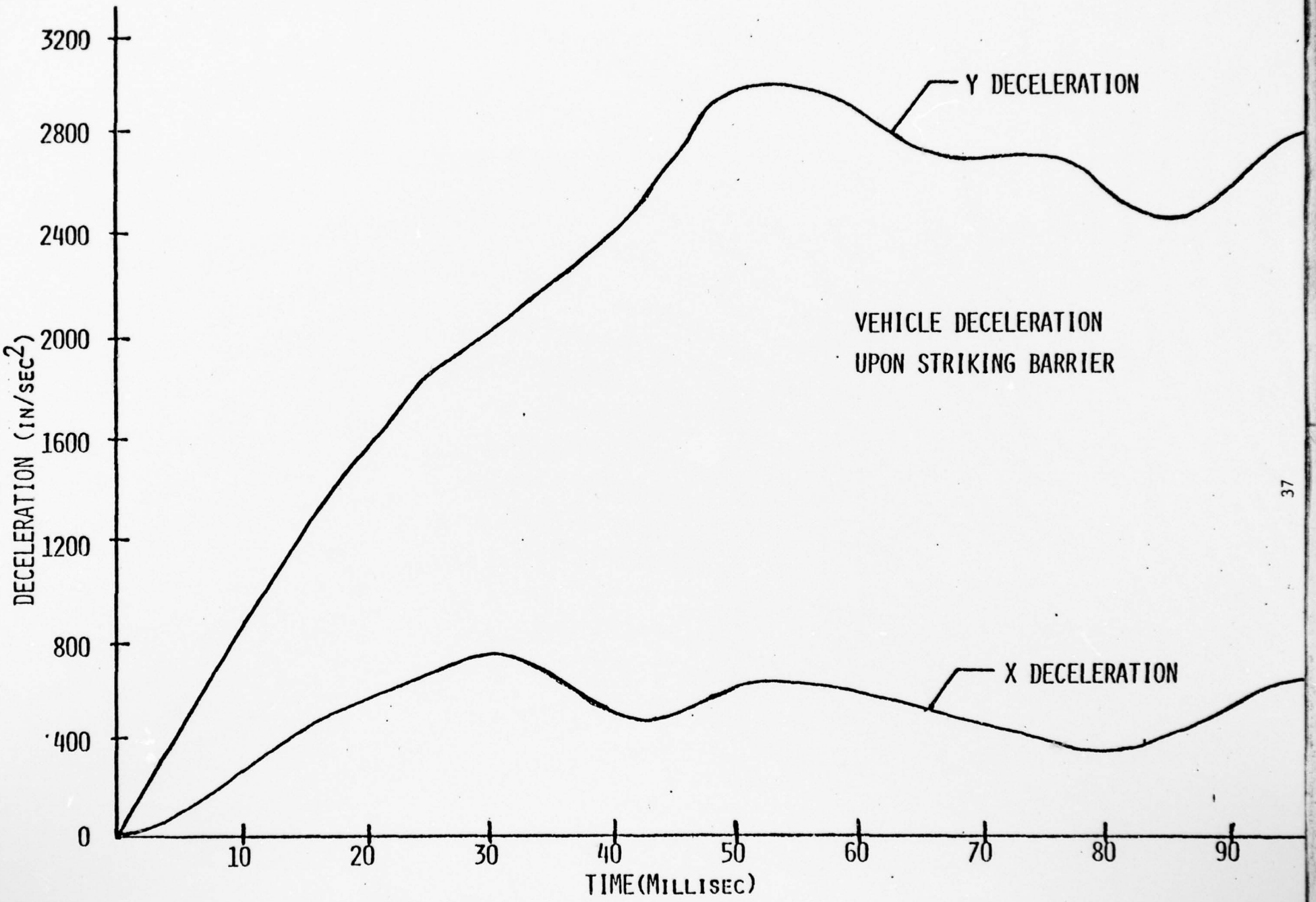

Figure 12. Vehicle Deceleration

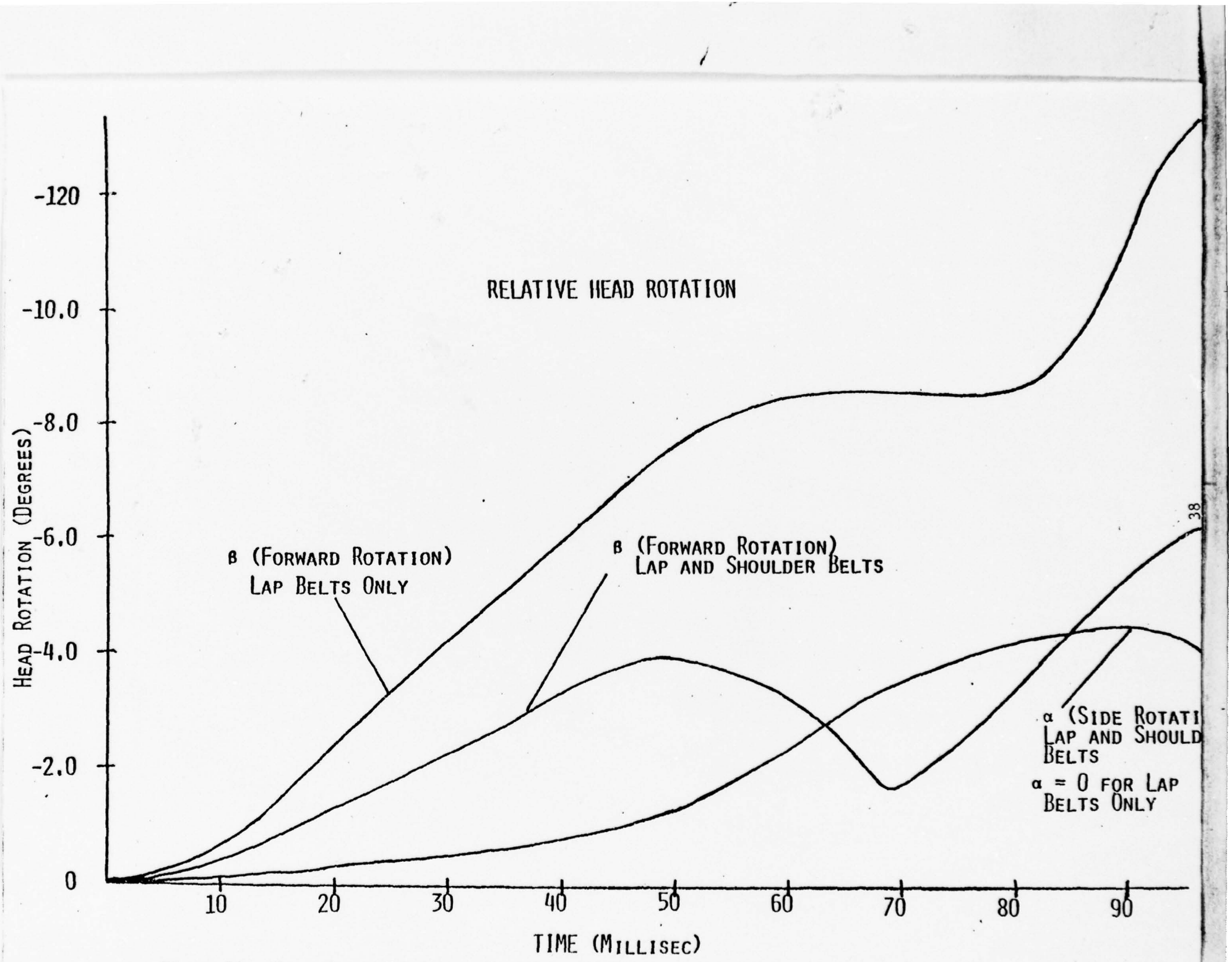

Figure 13. Comparison of Relative Head Rotation for Lap Belts and For a Combination of Lap and Shoulder Belts.

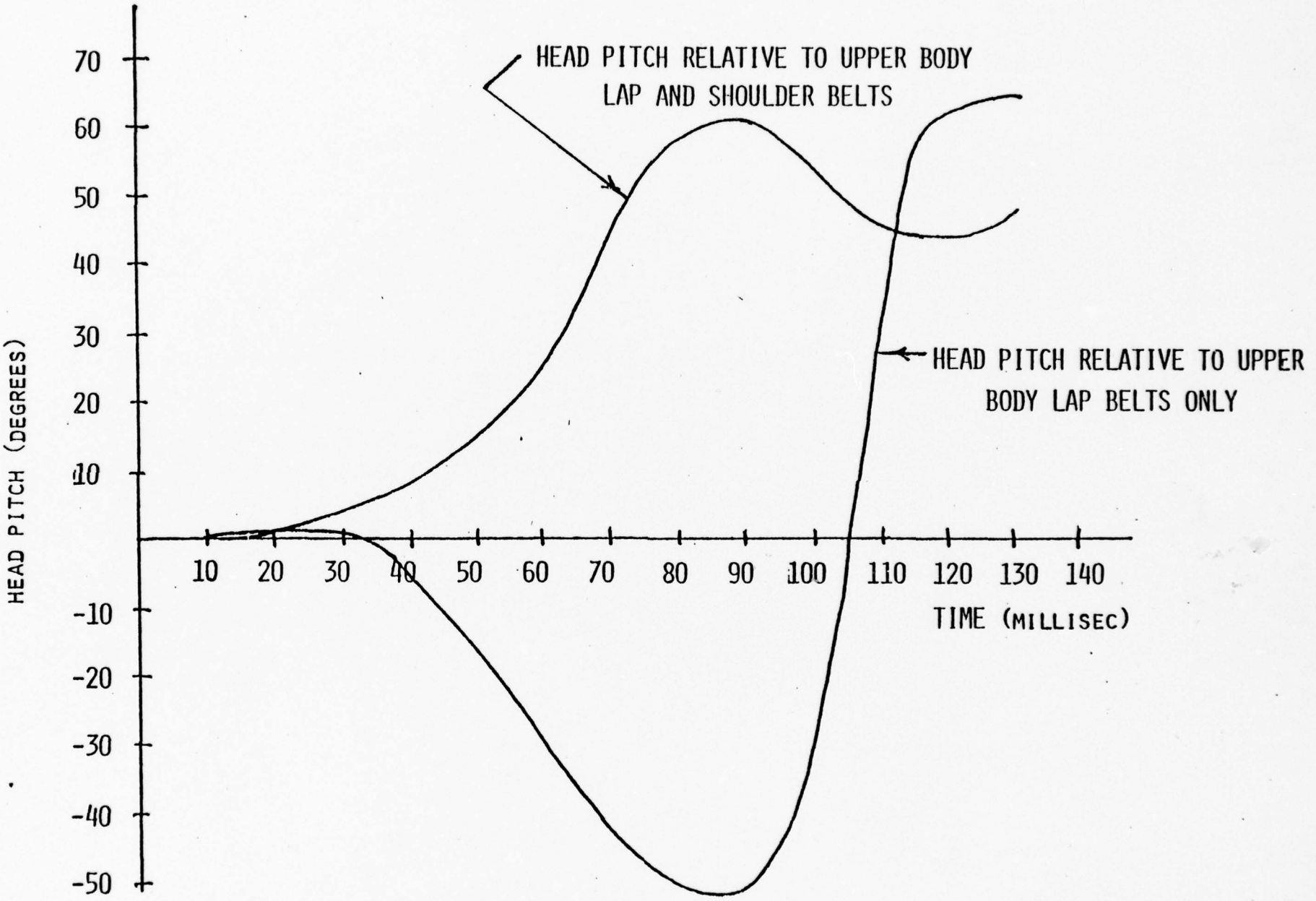

Figure 14. Comparison of Lap and Shoulder Belts (Front End Collision)

VI. APPLICATION WITH FINITE-SEGMENT CABLE MODELS

A second application area of the foregoing general analysis is the study of the dynamics of long, heavy cables. As with human body models, a finite-segment cable model is readily identified as a general chain system. Indeed, modelling a cable by a finite-segment model simply involves the substituting of a linked chain for the cable as shown in Figure 15. This model has the obvious advantage of being "linear", that is, not possessing any "branches". This in turn, provides a simplification in the governing equations.

Cable dynamics has been of interest to researchers for some time. But recently, with the advent of high-speed digital computers and finite-element methods and finite-segment modelling, there has been increasing interest and research effort in cable phenomena. Five years ago Choo and Casarella [82] published an excellent survey of the literature and analytical methods for cable dynamics. They indicate that of four methods for studying cable dynamics (the method of characteristics, the finite-element method, the linearization method, and the equivalent lumped mass method), the finite-element method is the most versatile. Indeed, they indicate that the finite-element or finite-segment method offers the best hope for a simple method that can solve nonlinear, unsteady state problems with good accuracy and yet require only a moderate amount of computation time.

References [83-92] provide a summary of recent finite-element and finite-segment approaches to cable dynamics. The approach in this report is to make a finite-segment model of the cable as in Figure 15. and to then follow the analysis as reported in Reference [93]. The basic dynamics of this model is then a specialization of the foregoing general theory.

Equations of Motion, Computer Code, and Numerical Solutions

The governing dynamical equations of motion are of the exact same form as those presented in Part IV of the Report. Indeed, the only modification required in the foregoing analysis is a simplification in the form of the mass center position and velocity expressions (due to the "linearity" of the cable model), and a specialization of the generalized active forces to account for the fluid drag forces.

Specifically, the expression for the position of the mass center of link B_k in Equation (3.14) is replaced with

$$\underset{\sim}{P}_k = (\xi_{oi}+SOK_{ih}r_{kh}+\sum_{M=1}^{k-1} SOM_{i\ell}\xi_{M\ell})\underset{\sim}{n}_{oi} \tag{6.1}$$

Then the velocity of the mass center in R (Equation 3.15) becomes

$$\underset{\sim}{v}_k = (\dot{\xi}_{oi}+SOK_{ih}r_{kh}+\sum_{M=1}^{k-1} SO\dot{M}\xi_{M\ell})\underset{\sim}{n}_{oi} \tag{6.2}$$

This leads to the following expressions for the non-zero $v_{k\ell m}$ (replacing Equations (3117), (3.18) and (3.21))

$$v_{k\ell m} = \delta_{\ell m} \quad (k=1,\ldots,N;\ \ell,m=1,2,3) \tag{6.3}$$

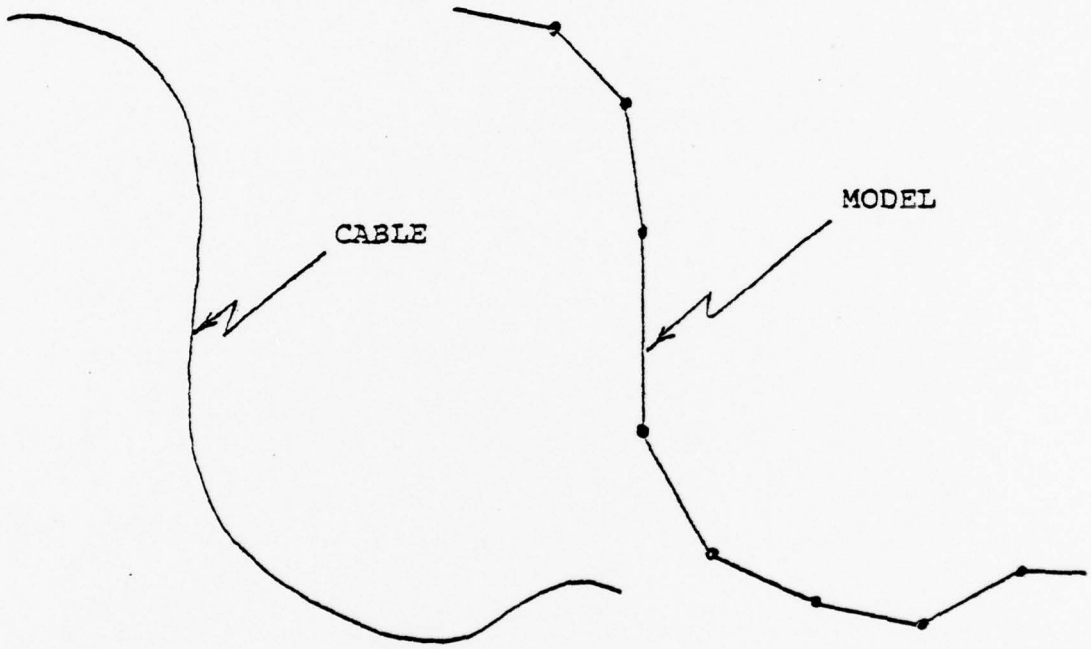

Figure 15. Finite-Segment Modelling of a Cable

$$v_{k\ell m} = WK_{mh\ell} r_{kh} + \sum_{M=1}^{k-1} WM_{mh\ell} \xi_{Mh} \tag{6.4}$$

$$(k=1,\ldots,N;\ \ell=1,\ldots,3N+3;\ m=1,2,3)$$

and

$$\dot{v}_{k\ell m} = W\dot{K}_{mh\ell} r_{kh} + \sum_{M=1}^{k-1} W\dot{M}_{mh\ell} \xi_{Mh} \tag{6.5}$$

$$(k=1,\ldots,N;\ \ell=1,\ldots,3N+3;\ m=1,2,3)$$

where N is the number of links or segments in the model.

Regarding the generalized active forces due to the fluid drag, the fluid forces on the cable links are modelled as follows: If B_k is a typical link, the fluid forces on B_k are taken to be equivalent to a single force $\underset{\sim}{F}_{kw}$ passing through G_k (the mass center of B_k) and perpendicular to the axis of B_k. (The axis is the line joining the connection points of B_{k-1}, B_k and B_k, B_{k+1} .) A sketch of $\underset{\sim}{F}_{kw}$ is given in Figure 16. Analytically $\underset{\sim}{F}_{kw}$ is expressed as

$$\underset{\sim}{F}_{kw} = -\rho A_k C_D |\underset{\sim}{v}_{k\perp}| \underset{\sim}{v}_{k\perp} \tag{6.6}$$

where ρ is the fluid mass density, A_k is the projected link area on a plane containing the axis of B_k, C_D is the drag coefficient, and

$$\underset{\sim}{v}_{k\perp} = \underset{\sim}{\lambda}_k \times [(\underset{\sim}{v}_k - \underset{\sim}{v}_w) \times \underset{\sim}{\lambda}_k] \tag{6.7}$$

where $\underset{\sim}{\lambda}_k$ is a unit vector parallel to the axis of B_k, $\underset{\sim}{v}_k$ is the velocity of G_k, and $\underset{\sim}{v}_w$ is the velocity of the fluid (See Figure 16.)

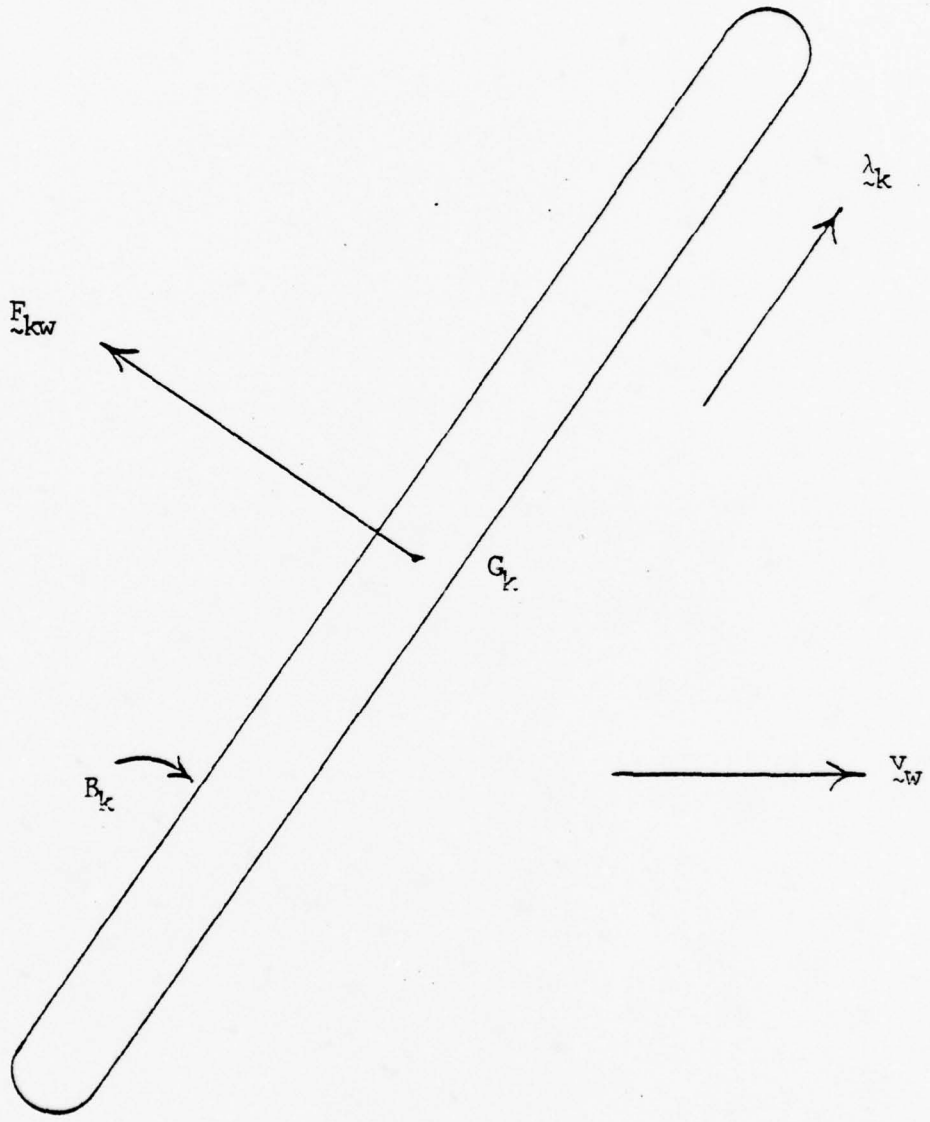

Figure 16. Fluid Force Model

To obtain the generalized active forces associated with the fluid drag (as well as the gravitational forces) $\underset{\sim}{F}_{kw}$ is substituted into Equation (4.1). This, in turn, leads to governing dynamical equation of motion of the form of Equations (4.7).

As with human-body crash-victim models, a computer code has been written to evaluate the coefficients of the governing equations. As input, the code requires: the number of links; the masses; the centroidal principal inertia matrices; the mass center positions; the connection point positions; the motion profile for those links with specified motion; the initial configuration; the ambient fluid velocity; the fluid surface height relative to R; the fluid mass density; the fluid kinematic viscosity; the projected link areas; the link diameters; and the mass densities of the links. The code provides for the evaluation of C_D, the drag coefficient of Equation (6.6) from an algorithm which models Hoerner's [94] drag coefficient curve.

The governing equations of motion are numerically integrated using a fourth order Runge-Kutta technique. The output of the computer code then includes: the values of all variables and their first derivatives; the connection point positions; the mass center positions; the mass center velocities and accelerations; and the moments and forces associated with the specified variables. All of the output is given at arbitrarily spaced time intervals.

Example Application

Consider a rotating surface crane with a 25 ft. boom dragging a 50 ft. cable attached to a submerged 1 ft. diameter sphere, as depicted in Figure 17.* The cable is modelled by 10 cylindrical links, each 5 ft. long. The cable diameter is 1 in. and each link has a mass of 0.4025 slug. The sphere mass is 7.727 slug. The water is calm and its surface is 10 ft. below the boom.

The boom makes a 90° turn in 5 sec. The angular acceleration is given by the graph in Figure 18. The resultant motion of the sphere is shown in Figures 19. and 20. To determine the effect of the water drag force, the same run without the water. It is seen (as one would expect) that the drag forces tend to counteract the inertia forces.

---

* Although this simulates an off-shore oil rig or a ship's crane, it does not represent any specific physical situation. Indeed, the intention is simply to demonstrate the kinds of problems which can be studied with the above described analysis and computer code.

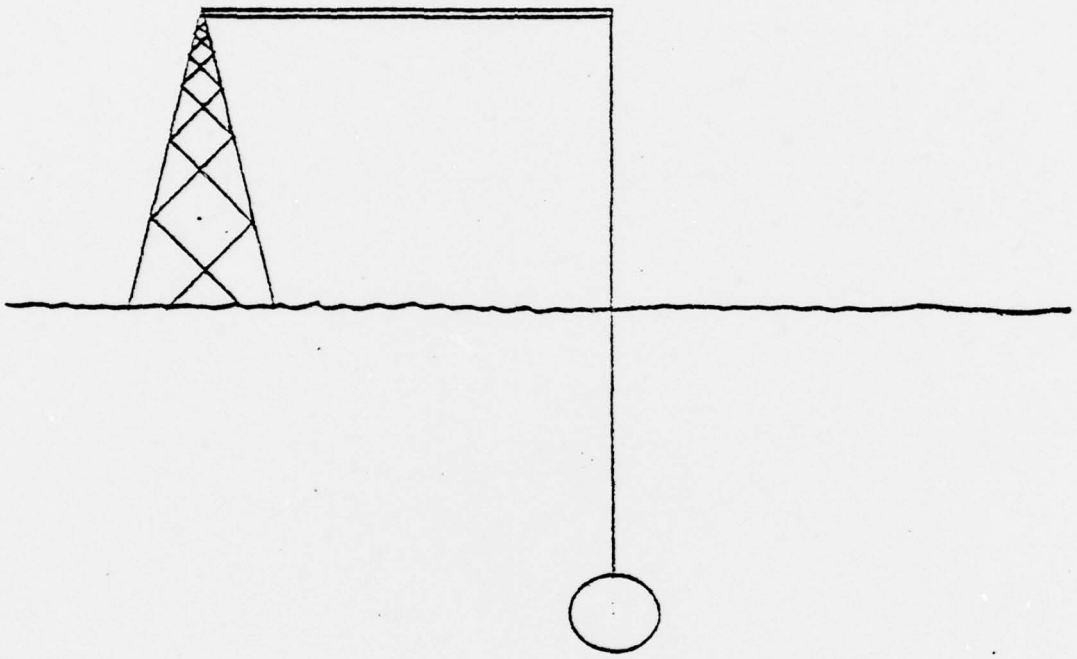

Figure 17. Boom, Cable and Submerged Sphere

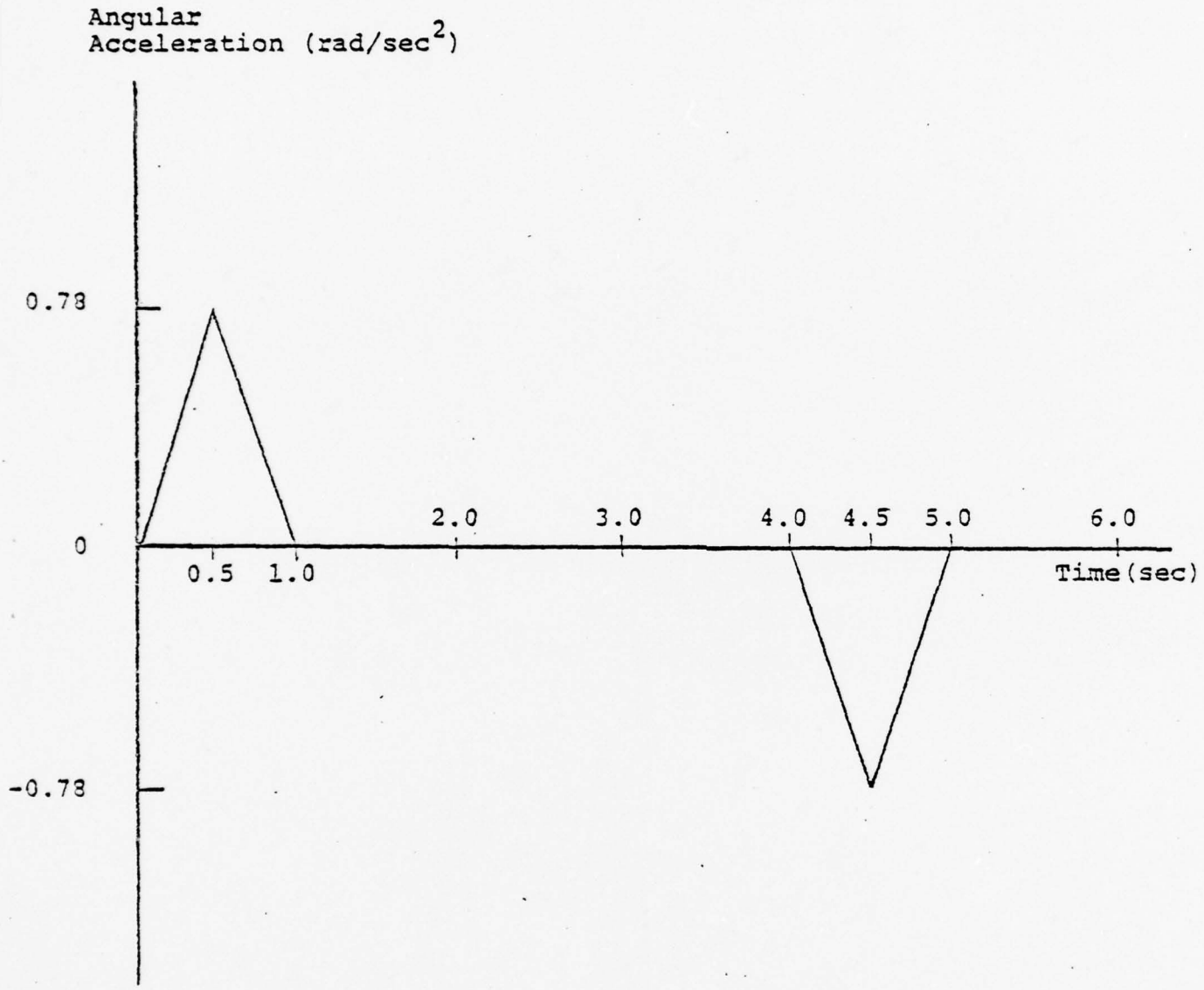

Figure 18. Angular Acceleration of the Boom

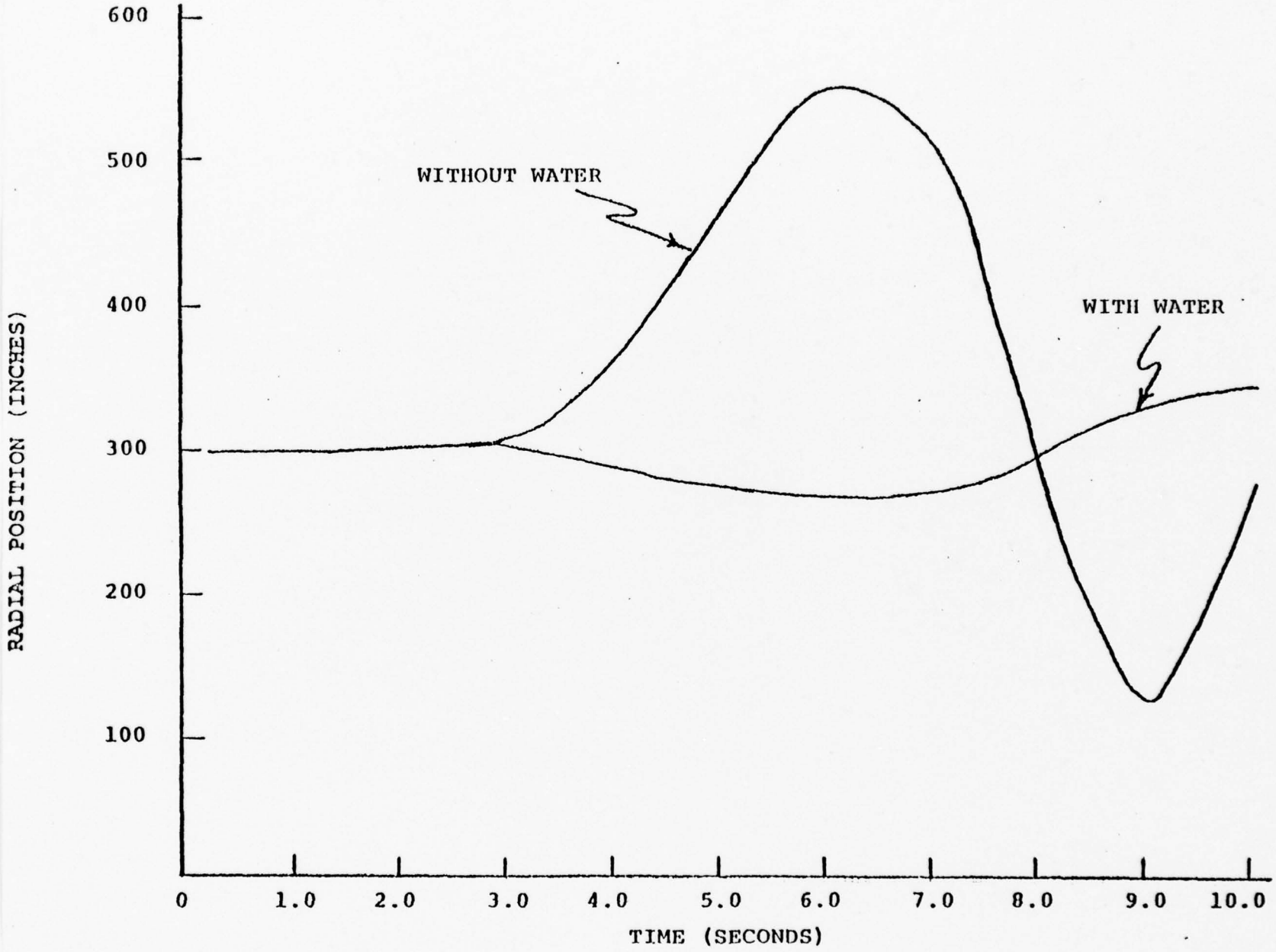

Figure 19. Radial Position of the Sphere

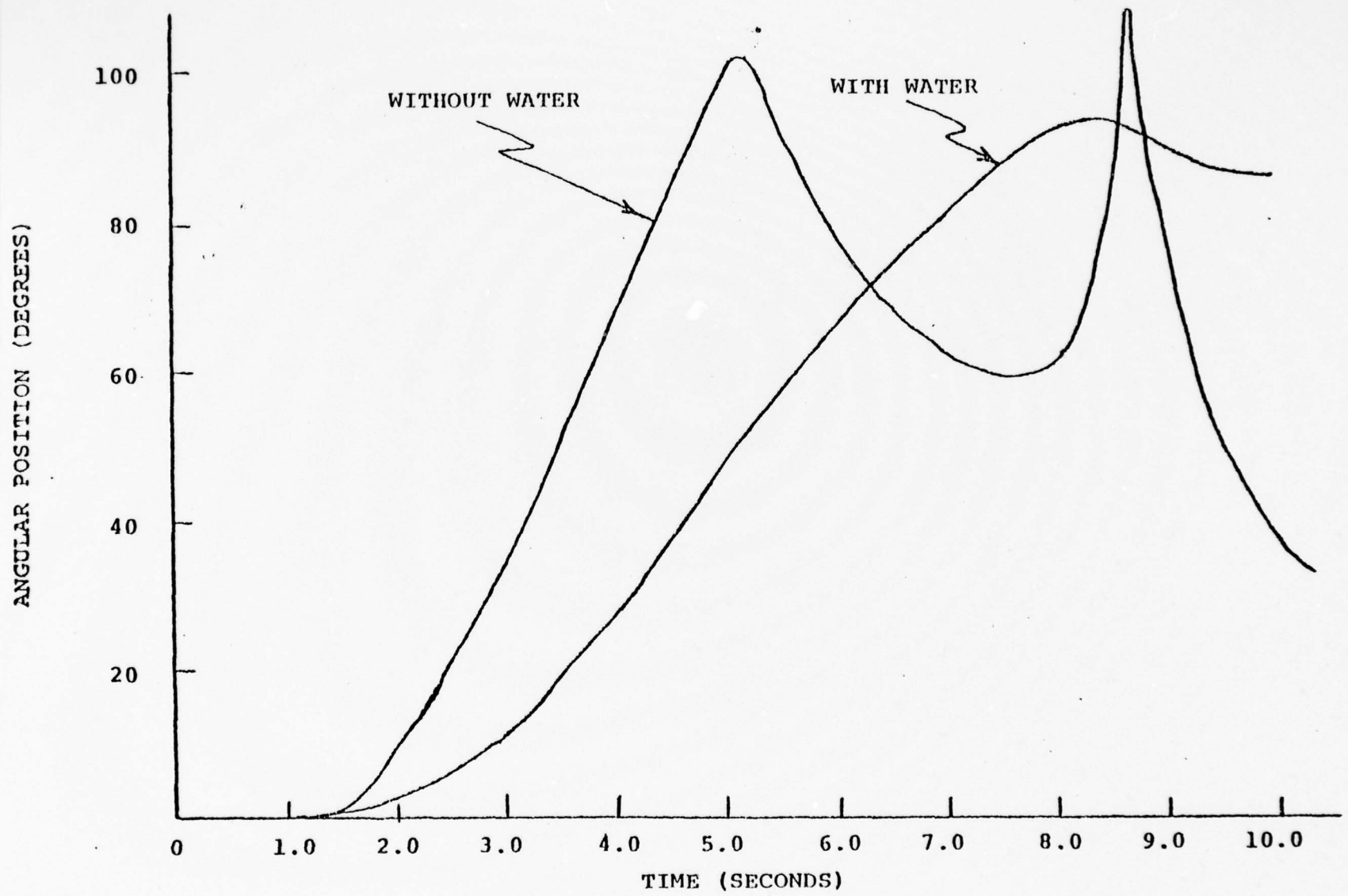

Figure 20. Angular Positions of the Sphere

VII. DISCUSSION AND CONCLUSIONS

A new, efficient, computer-oriented method for obtaining equations of motion for large mechanical systems (chain systems) has been developed. These equations may be succinctly written in the form of Equations (4.7) with the coefficients determined by the four kinematical matrices $\omega_{k\ell m}$, $\dot{\omega}_{k\ell m}$, $v_{k\ell m}$, and $\dot{v}_{k\ell m}$. These matrices, in turn are determined by simple multiplication algorithms which enable the entire procedure to be reduced to a systematic routine.

The development of this method was made possible through the use of Lagrange's form of d'Alembert's principle which provides for the automatic elimination of non-working constraint forces. Specifically, it is this feature, combined with the use of vector-matrix notational schemes, which make possible the explicit writing of the equations of motion. Also, the analysis makes use of "local" as opposed to "global" coordinates. That is, the generalized coordinates of the system are (except for the translation of the first body (or segment) relative orientation angles measured between the respective bodies as opposed to absolute orientation angles of the bodies (or segments) in space. This allows for a more convenient specification of initial conditions and constraints, and for a more convenient interpretation of the results.

The range of application of the analysis and procedures is very broad. The two example areas of human-body models and cable models are simply two areas where there is current interest. Information regarding other possible areas of application, the use

of program tapes, and user manuals may be obtained from the authors.

Future work will involve extending the procedures to allow for translation between the bodies and for closed loops in the system models.

REFERENCES

1. Hooker, W. W., and Margulies, G., "The Dynamical Attitude Equations for an n-Body Satellite", Journal of the Astronatuical Sciences, Vol. XII, No. 4, 1965, pp. 123-128.

2. Roberson, R. E., and Wittenburg, J., "A Dynamical Formalism for an Arbitrary Number of Interconnected Rigid Bodies, with Reference to the Problem of Attitude Control", Proceedings of the 3rd International Congress of Automatic Control, Butterworth, London, 1967, pp. 46D.1-46D.8.

3. Hooker, W. W., "A Set of r Dynamical Attitude Equations for an Arbitrary n-Body Satellite Having r Rotational Degrees of Freedom", AIAA Journal, Vol. 8., No. 7., 1970, pp. 1205-1207.

4. Chace, M. A., and Bayazitoglu, Y. O., "Development and Application of a Generalized d'Alembert Force for Multifreedom Mechanical Systems", Journal of Engineering for Industry, Vol. 93., 1971, pp. 317-327.

5. Bayazitoglu, Y. O., "Methods for Automated Analysis of Three-Dimensional Mechanical Dynamic Systems with Application to Nonlinear Vehicle Dynamics", Ph.D. Dissertation, University of Michigan, 1972.

6. Fleischer, G. E., "Multi-Rigid-Body Attitude Dynamics Simulator", JPL Technical Report No. 32-1516, 1971.

7. Likins, P. W., "Finite Element Appendage Equations for Hybrid Coordinate Dynamic Analysis", International Journal of Solids and Structures, Vol. 8., 1972, pp. 709-731.

8. Passerello, C. E., and Huston, R. L., "An Analysis of General Chain Systems", NASA-CR-127924, Report No. N72-30532, 1972.

9. Likins, P. W., "Dynamic Analysis of a System of Hinge Connected Rigid Bodies with Non-rigid Appendages", International Journal of Solids and Structures, Vol. 9., 1973, pp. 1473-1487.

10. Huston, R. L., and Passerello, C. E., "On the Dynamics of Chain Systems", ASME Paper No. 74-WA/Aut.11, ASME Winter Annual Meeting, New York, 1974.

11. Hooker, W. W., "Equations of Motion for Interconnected Rigid and Elastic Bodies", Celestial Mechanics, Vol. 11, No. 3., May, 1975 pp. 337-359.

12. Huston, R. L., and Passerello, C. E., "Dynamics of General Chain Systems", NTIS Report PB257184, August, 1976.

13. Jerkovsky, W., "The Transformation Operator Approach to Multi-Systems Dynamics Part I: The General Approach", The Matrix and Tensor Quarterly, Vol. 27., No. 2., December, 1976, pp. 48-59.

14. Kane, T. R., "Dynamics of Nonholonomic Systems", Journal of Applied Mechanics, Vol. 28., 1961, pp. 574-578.

15. Kane, T. R., and Wang, C. F., "On the Derivation of Equation of Motion", Journal of the Society for Industrial and Applied Mathematics, Vol. 13., 1965, pp. 487-492.

16. Kane, T. R., Dynamics, Holt, Rinehart, and Winston, New York, 1968.

17. Huston, R. L., and Passerello, C. E., "On Lagranges Form of d'Alembert's Principle", The Matrix and Tensor Quarterly, Vol. 23., No. 3., March, 1973, pp. 109-112.

18. Passerello, C. E., and Huston, R. L., "Human Attitude Control", Journal of Biomechanics, Vol. 4., 1971, pp. 95-102.

19. Huston, R. L., and Passerello, C. E., "On the Dynamics of a Human Body Model", Journal of Biomechanics, Vol. 4., 1971, pp. 369-378.

20. Eringen, A. C., Nonlinear Theory of Continuous Media, McGraw Hill, New York, 1962.

21. Kane, T. R. and Likins, P. W., "Kinematics of Rigid Bodies in Spaceflight", Stanford University, Department of Applied Mechanics, Technical Report No. 204, 1971.

22. Brand, L., Vector and Tensor Analysis, Wiley, New York, 1947.

23. Kane, T. R., Analytical Elements of Mechanics, Vol. 2. Dynamics, Academic Press, New York, 1961.

24. Huston, R. L., Hessel, R. E., and Passerello, C. E., "A Three Dimensional Vehicle-Man Model for Collision and High Acceleration Studies", Paper No. 740275, Society of Automotive Engineers, 1974.

25. Huston, R. L., Hessel, R. E., and Winget, J. M., "Dynamics of a Crash Victim -- A Finite Segment Model", AIAA Journal, Vol. 14., No. 2., 1976, pp. 173-178.

26. Huston, R. L., Passerello, C. E., Harlow, M. W., and Winget, J. M., "The UCIN 3-Dimensional Aircraft Occupant", Aircraft Crashworthiness, University Press of Virginia, 1975, pp. 311-324.

27. Huston, R. L., Passerello, C. E., and Harlow, M. W., "User's Manual for UCIN Vehicle-Occupant Crash Study Model--Version II", ONR Contract Report No. ONR-UC-EA-120/74-3, 1974.

28. Huston, R. L., Passerello, C. E., and Harlow, M. W., "UCIN Vehicle-Occupant/Crash Victim Simulation Model", Structural Mechanics Software Series, University Press of Virginia, 1977.

29. Huston, R. L., Passerello, C. E., Hessel, R. E., and Harlow, M. W., "On Human Body Dynamics", Annals of Biomedical Engineering, Vol. 4., 1976, pp. 25-43.

30. King, A. I., and Chou, C. C., "Mathematical Modelling, Simulation and Experimental Testing of Biomechanical System Crash Response", Journal of Biomechanics, Vol. 9., No. 5., 1976, pp. 301-317.

31. Robbins, D. H., "Simulation of Human Body Response to Crash Loads", Shock and Vibration Computer Programs--Reviews and Summaries, The Shock and Vibration Information Center, Naval Research Laboratory, Washington, D. C., 1975, pp. 365-380.

32. Huston, R. L., "Three-Dimensional, Gross-Motion, Crash-Victim Simulators", Structural Mechanics Software Series, University Press of Virginia, 1975.

33. King, A. I., "Survey of the State of the Art of Human Biodynamic Response", Aircraft Crashworthiness, University Press of Virginia, 1975, pp. 83-120.

34. Smith, P. G., and Kane, T. R., "On the Dynamics of the Human Body in Free Fall", Journal of Applied Mechanics, Vol. 35., 1968, p. 167.

35. Kane, T. R., and Scher, M. P., "Human Self-Rotation by Means of Limb Movements", Journal of Biomechanics, Vol. 3., 1970, pp. 33-49.

36. Gallenstein, J., and Huston, R. L., "Analysis of Swimming Motions", Human Factors, Vol. 15., 1973, pp. 91-98.

37. Abdelnour, T. A., Passerello, C. E., and Huston, R. L., "An Analytical Analysis of Walking", ASME Paper No. 75-WA/Bio-4, American Society of Mechanical Engineers, Winter Annual Meeting, 1975.

38. Ghosh, T. K., and Boykin, W. H., Jr., "Analytical Determination of an Optimal Human Motion", Journal of Optimization Theory and Applications, Vol. 19., 1976, pp. 327-346.

39. McHenry, R. R., "Analysis of the Dynamics of Automobile Passenger Restraint Systems", Proceedings of the 7th Stapp Car Crash Conference, 1963, pp. 207-249.

40. McHenry, R. R. and Naab, K. N., "Computer Simulation of the Automobile Crash Victim--A Validation Study", Cornell Aeronautical Laboratories, Inc., Report No. YB-2126-V-1R, July, 1966.

41. McHenry, R. R., and Naab, K. N., "Computer Simulation of the Crash Victim--A Validation Study", Proceedings of the 10th Stapp Car Crash Conference, Holloman AFB N.M., 1966.

42. McHenry, R. R., Naab, K. N., et.al., "Cal Computer Simulation Predicts Occupant Responses During Vehicle Head-On Collision", SAE Journal, Vol. 75., No. 7., July, 1967, pp. 36-45.

43. Segal, D. J., and McHenry, R. R., "Computer Simulation of the Automobile Crash Victim-Revision No. 1.", Cornell Aeronautical Laboratories, Inc., Report No. VJ-2492-V-1, March, 1968.

44. Segal, D. J., "Revised Computer Simulation of the Automobile Crash Victim", Cornell Aeronautical Laboratories, Inc., Report No. VJ-2759-V-2, Jan. 1971.

45. Segal, D. J., "Computer Simulation of Pedestrial Accidents", Third Triennial Congress of the International Association for Accident and Traffic Medicine, New York, N.Y., 1969.

46. Danforth, J. P., and Randall, C. D., "Modified ROS Occupant Dynamics Simulation User Manual", General Motors Corp. Research Labs., Publication No. GMR-1254, Oct., 1972.

47. Glancy, J. J. and Larsen, S. E., "User Guide for Program SIMULA", Dynamic Science, Report TDR No. 72-23, 1972.

48. Karnes, R. N., Sebastian, J. D., Tocher, J. L., and Twigg, D. W., "A User-Oriented Program for Crash Dynamics", Proceedings of the International Conference on Vehicle Structural Mechanics, Detroit, Mich., March, 1974, pp. 154-163.

49. Twigg, D. W., and Karnes, R. N., "PROMETHEUS--A User Oriented Program for Human Crash Dynamics (User Manual)", ONR Contract N00014-72-C-0223, Report No. BCS-40038, Nov., 1974.

50. Karnes, R. N., Tocher, J. L., and Twigg, D. W., "PROMETHEUS--A Crash Victim Simulator", Aircraft Crashworthiness, University Press of Virginia, 1975, pp. 327-345.

51. Collins, J. A., and Turnbow, J. W., "Response of A Seat-Passenger System", Symposium on Dynamic Response of Structures, Stanford Univ., Stanford, CA., June 1971.

52. Robbins, D. H., Bennett, R. O., and Roberts, V. L., "HSRI Two-Dimensional Crash Victim Simulator: Analysis, Verification, and Users' Manual", NTIS Report No. PB202 537, Dec. 1970.

53. Bowman, B. M., Bennett, R. O., and Robbins, D. H., "MVMA Two-Dimensional Crash Victim Simulation, Version 3", 3 Volume Report, NTIS Nos. 235 753/1, 236 907/2, 236 908/0, June, 1974.

54. Robbins, D. H., Bowman, B. M., and Bennett, R. O., "The MVMA Two-Dimensional Crash Victim Simulation", Proceedings of the 18th Stapp Car Crash Conference, Warrendale, Pa., 1974.

55. Robbins, D. H., Bennett, R. O., and Bowman, B. M., "User-Oriented Mathematical Crash Victim Simulator", Proceedings of the 16th Stapp Car Crash Conference, Warrendale, Pa., 1972, pp. 128-148.

56. Robbins, D. H., Bennett, R. O., and Roberts, V. L., "HSRI Three-Dimensional Crash Victim Simulator: Analysis, Verification, Users' Manual, and Pictorial Section", NTIS Report No. PB 208 242, June, 1971.

57. Robbins, D. H., "Three-Dimensional Simulation of Advanced Automotive Restraint Systems", Paper No. 700421, 1970, International Automobile Safety Conference Compendium, p-30 SAE, Warrendale, Pa., May, 1970, pp. 1008-1023.

58. King, A. I., Chou, C. C., Mackinder, J. A., "Mathematical Model of an Airbag for a Three-Dimensional Occupant Simulation", SAE Paper No. 720036, Warrendale, Pa., Jan. 1971.

59. Patrick, L. M., "Airbag Restraint for Automobile Drivers, Vol. II, Occupant Simulation Model", Final Report on DOT Contract FH-11-7607 for NHTSA, Wayne State University, Detroit, Mich., 1972.

60. Robbins, D. H., Bennett, R. O., and Bowman, B. M., "HSRI Six-Mass, Three-Dimensional Crash Victim Simulator", NTIS Report No. PB 239 476, Feb., 1973.

61. Young. R. D., "A Three-Dimensional Mathematical Model of an Automobile Passenger", Research Report 140-2, Texas Transportation Institute, Texas A and M University, College Station, Tex. NTIS Report No. PB 197 159, Aug., 1970.

62. Young, R. D., Ross, H. E., and Lammert, W. F., "Simulation of the Pedestrian During Vehicle Impact", Proceedings of the 3rd International Congress on Automotive Safety, Paper No. 27, Vol. II, 1974.

63. Young, R. D., "Vehicle Exteriors and Pedestrial Injury Prevention, Vol. V, A Three-Dimensional Mathematical Simulation--Extension and Validation", Final NHTSA Contract Report, Texas Transportation Institute, College Station, Texas, 1975.

64. Laananen, D. H., "A Digital Simulation Technique for Crashworthy Analysis of Aircraft Seats", SAE Paper No. 740371, Warrendale, Pa., April, 1974.

65. Laananen, D. H., "Development of a Scientific Basis for Analysis of Aircraft Seating Systems", Report No. FAA-NA-74-175, Ultrasystems, Inc., Dynamic Science Div., Phoenix, AZ., Jan., 1975.

66. Laananen, D. H., "Implementation of a Digital Simulation Technique for Crashworthy Analysis of Aircraft Seats", Presentation 750541 at the SAE Business Aircraft Meeting, Wichita, KS., April, 1975.

67. Laananen, D. H., "Simulation of an Aircraft Seat and Occupant in a Crash Environment", Aircraft Crashworthiness, University Press of Virginia, 1975, pp. 347-363.

68. Bartz, J. A., "A Three-Dimensional Computer Simulation of a Motor Vehicle Crash Victim, Phase II, Validation Study of the Model", CAL Report No. VJ-2978-V-2, Calspan Corp., Buffalo, N.Y., Dec., 1972.

69. Fleck, J. T., Butler, F. E., and Vogel, S. L., "An Improved Three-Dimensional Computer Simulation of Motor Vehicle Crash Victims", Cal Report No. ZQ-5180-L-1, Calspan Corp., Buffalo, N.Y., 1974.

70. Karnes, R. N., "CAL 3D Crash Victim Simulation Computer Program User Manual", Document No. BCS-G0651, Boeing Computer Services, Inc., Seattle, Wash., March, 1971.

71. Fleck, J. T., "CALSPAN Three-Dimensional Crash Victim Simulation Program", Aircraft Crashworthiness, University Press of Virginia,

72. Begeman, P. C., King, A. I., and Prasad, P., "Spinal Loads Resulting From - G_x Acceleration", Proceedings of the 17th Stapp Car Crash Conference, Warrendale, Pa., 1973, pp. 343-360.

73. Ewing, C. L., and Thomas, D. J., "Response of Human Head to Impact", Proceedings of the 17th Stapp Car Crash Conference, Warrendale, Pa., 1973, pp. 309-342.

74. Ewing, C. L., Thomas, D. J., Patrick, L. M., Beeler, G. W., and Smith, M. J., "Living Human Dynamic Response to - G_x Impact Acceleration II - Accelerations Measured on the Head and Neck", Proceedings of the 13th Stapp Car Crash Conference, Warrendale, Pa., 1969, pp. 400-415.

75. Ewing, C. L., and Thomas, D. J., "Human Head and Neck Response to Impact Acceleration", Army-Navy Joint Report, Naval Aerospace Medical Research Laboratory, J. S. Army Aeromedical Research Laboratory, Monograph 21, Aug., 1972.

76. Furusho, H., Yokoya, K., and Fujiki, S., "Dynamics of Occupants in Collision: Vol. 1, Simulation of 3-D Man Model with Five Masses", Society of Mechanical Engineers of Japan, Western Division Meeting Reprint, 1970.

77. Furusho, H., and Yokoya, K., "Analysis of Occupants Movement in Head-On Collision", Transactions of the Society of Automotive Engineers of Japan, No. 1, 1970, pp. 145-155.

78. Furusho, H., Yokoya, K., and Fujiki, S., "Analysis of Occupant Movements in Rear-End Collision", Paper No. 13 of Safety Research Tour in the U.S.A. from the Viewpoint of Vehicle Dynamics, 1969.

79. King, A. I., Padgaonkar, A. J., and Mital, N. K., "Measurement and Prediction of Occupant Response: Spine, Thorax and Whole-Body", Measurement and Prediction of Structural and Biodynamic Crash-Impact Response, Saczalski, K. J., and Pilkey, W. D. editors, ASME, 1976, pp. 97-119.

80. Begeman, P. C., King, A. I., and Prasad, P., "Spinal Loads Resulting from - G_x Acceleration", Proceedings of the 17th Stapp Car Crash Conference, 1973, pp. 343-360.

81. Powell, G. H., "Computer Evaluation of Automobile Barrier Systems", Federal Highway Administration, Report No. FHWA-RD-73-73, 1970.

82. Choo, Y., and Casarella, M. J., "A Survey of Analytical Methods for Dynamic Simulation of Cable-Body Systems", Journal of Hydronautics, Vol. 7., 1973, pp. 137-144.

83. Elnan, O., and Evert, C., "Dynamics of a Tethered Balloon in the Longitudinal Plane", Goodyear Aerospace Report GER-12901, 1966.

84. Morgan, B. J., "The Finite Element Method and Cable Dynamics", Proceedings of the Symposium on Ocean Engineering, Paper 3C, University of Pennsylvania, 1970.

85. Leonard, J. W., "Curved Finite Element Approximation to Nonlinear Cables", Offshore Technology Conference, Paper OTC 1533, Houston, Texas, 1972.

86. Leonard, J. W., "Nonlinear Dynamics of Curved Cable Elements", Journal of the Engineering Mechanics Division, Proceedings ASCE, Vol. 99, 1973, pp. 616-621.

87. Paul, B., and Soler, A. I., "Cable Dynamics and Optimum Touring Strategies for Submersibles", Marine Technology Society Journal, Vol. 6, 1972, pp. 34-42.

88. Hicks, J. B. and Clark, L. B., "On the Dynamic Response of Bony-Supported Cables and Pipes to Currents and Waves", Offshore Technology Conference, Paper OTC 1556, Houston, Texas, 1972.

89. Doninguez, R. F., and Smith, D. E., "Dynamic Analysis of Cable Systems", Journal of the Structures Division, Proceedings ASCE, Vol. 98., 1972, pp. 1817-1834.

90. Crist, S. A., "Analysis of the Motion of a Long Wire Towed from an Orbiting Aircraft", Shock and Vibration Bulletin No. 41-Pt.6, Naval Research Lab., 1970.

91. Walton, T. W., and Polachek, H., "Calculation of Transient Motion of Submerged Cables", Mathematical Tables and Aids to Computation, Vol. 14., 1960, pp. 27-60.

92. Strandhagen, A. G., and Thomas, C. F., "Dynamics of Towed Underwater Vehicles", Navy Mine Defense Lab, Panama City, Fla., Report No. 219., 1963.

93. Winget, J. M., and Huston, R. L., "Cable Dynamics--A Finite Segment Approach", Journal of Computers and Structures, Vol. 6., 1976, pp. 475-480.

94. Hoerner, S. F., Fluid Dynamic Drag, Hoerner, New York, 1965.

ONR DISTRIBUTION LIST

Part I - Government

Chief of Naval Research
Department of the Navy
Arlingon, Virginia 22217
Attn: Code 474 (2)
471
222

Director
ONR Branch Office
495 Summer Street
Boston, Massachusetts 02210

Director
ONR Branch Office
536 S. Clark Street
Chicago, Illinois 60604

Director
Naval Research Laboratory
Attn: Code 2529 (ONRL)
Washington, D.C. 20390 (6)

U.S. Naval Research Laboratory
Attn: Code 2627
Washington, D.C. 20390

Commanding Officer
ONR Branch Office
207 West 24th Street
New York, N.Y. 10011

Director
ONR Branch Office
1030 E. Green Street
Pasadena, California 91101

Defense Documentation Center
Cameron Station
Alexandria, Virginia 22314 (12)

Army

Commanding Officer
U.S. Army Research Off. Durham
Attn: Mr. J. J. Murray
CRD-AA-IP
Box CM, Duke Station
Durham, North Carolina 27706

Commanding Officer
AMXMR-ATL
Attn: Mr. R. Shea
U.S. Army Materials Res. Agency
Watertown, Massachusetts 02172

Watervliet Arsenal
MAGGS Research Center
Watervliet, New York 12189
Attn: Director of Research

Redstone Scientific Info. Center
Chief, Document Section
U.S. Army Missile Command
Redstone Arsenal, Alabama 35809

Army R &D Center
Fort Belvoir, Virginia 22060

Navy

Commanding Officer & Director
Naval Ship Res. & Dev. Center
Bethesda, Maryland 20034
Attn: Code 042 (Tech. Lib. Br.)
17 (Struc. Mech. Lab.)
172
172
174
177
1800(Appl. Math. Lab.)
5412S (Dr. W.D. Sette)
19 (Dr. M.M. Sevik)
1901 (Dr. M. Strassberg)
1945
196 (Dr. D. Feit)
1962

Naval Weapons Laboratory
Dahlgren, Virginia 22448

Naval Research Laboratory
Washington, D.C. 203
Attn: Code 8400
8410
8430
8440
6300
6390
6380

Undersea Explosion Res. Div.
Naval Ship R&D Center
Norfolk Naval Shipyard
Portsmouth, Virginia 23709
Attn: Dr. E. Palmer
Code 780

Naval Ship Res. & Dev. Center
Annapolis Division
Annapolis, Maryland 21402
Attn: Code 2740 - Dr. Y. F. Wang
28 - Mr. R.J. Wolfe
281 - Mr. Niederberger
2814 - Dr. H. Vandervelde

Technical Library
Naval Underwater Weapons Center
Pasadena Annex
3202 E. Foothill Blvd.
Pasadena, California 91107

U.S. Naval Weapons Center
China Lake, California 93557
Attn: Code 4062 - Mr. W. Werback
4520 - Mr. Ken Bischel

Commanding Officer
U.S. Naval Civil Engr. Lab.
Code L31
Port Hueneme, California 93041

Technical Director
U.S. Naval Ordnance Lab.
White Oak
Silver Spring, Maryland 20910

Technical Director
Naval Undersea R&D Center
San Diego, California 92132

Supervisor of Shipbuilding
U.S. Navy
Newport News, Virginia 23607

Techanical Director
Mare Island Naval Shipyard
Vallejo, California 94592

U.S. Navy Underwater Sound Ref. Lab.
Office of Naval Research
P.O. Box 8337
Orlando, Florida 32806

Chief of Naval Operations
Dept. of the Navy
Washington, D.C. 20350
Attn: Code Op07T

Strategic Systems Project Off.
Department of the Navy
Washington, D.C. 20390
Attn: NSP- 001 Chief Scientist

Deep Submergance Systems
Naval Ship Systems Command
Code 39522
Department of the Navy
Washington, D.C. 203 60

Engineering Dept.
U.S. Naval Academy
Annapolis, Maryland 21402

Naval Air Systems Command
Dept. of the Navy
Washington, D.C. 20360
Attn: NAVAIR 5302 Aero & Struc.
5308 Struc.
52031F Materials
604 Tech. Lib.

Director, Aero Mechanics
Naval Air Development Center
Johnsville
Warminster, Pennsylvania 18974

Technical Director
U.S. naval Undersea R&D Center
San Diego, California 92132

Engineering Department
U.S. Naval Academy
Annapolis, Maryland 21402

Naval Facilities Engineering Command
Dept. of the Navy
Washington, D.C. 20360
Attn: NAVFAC 03 Res. & Dev.
04 Res. & Dev.
14114 Tech. Lib.

Naval Sea Systems Command
Dept. of the Navy
Washington, D.C. 20360
Attn: NAVSHIP 03 Res. & Tech.
031 Ch.Scientist R&D
03412 Hydromechanics
037 Ship Silencing Div.
035 Weapons Dynamics

Navy cont.

Naval Ship Engineering Center
Prince George's Plaza
Hyattsville, Maryland 20782
Attn: NAVSEC 6100 Ship Sys Engr & Des Dep
6102C Computer-Aided Ship Des
6105G
6110 Ship Concept Des
6120 Hull Div.
6120D Hull Div.
6128 Surface Ship Struct.
6129 Submarine Struct.

Air Force

Commander WADD
Wright-Patterson Air Force Base
Dayton, Ohio 45433
Attn: Code WWRMDD
AFFDL (FDDS)
Structures Division
AFLC (MCEEA)

Chief, Applied Mechanics Group
U.S. Air Force Inst. of Tech.
Wright-Patterson Air Force Base
Dayton, Ohio 45433

Chief, Civil Engineering Branch
WLRC, Research Division
Air Force Weapons Laboratory
Kirtland AFB, New Mexico 87117

Air Force Office of Scientific Research
1400 Wilson Blvd.
Arlington, Virginia 22209
Attn: Mechanics Div.

NASA

Structures Research Division
National Aeronautics & Space Admin.
Langley Research Center
Langley Station
Hampton, Virginia 23365

National Aeronautic & Space Admin.
Associate Administrator for Advanced Research & Technology
Washington, D.C. 02546

Scientific & Tech. Info. Facility
NASA Representative (S-AK/DL)
P.O. Box 5700
Bethesda, Maryland 20014

Other Government Activities

Commandant
Chief, Testing & Development Div.
U.S. Coast Guard
1300 E. Street, N.W.
Washington, D.C. 20226

Technical Director
Marine Corps Dev & Educ. Command
Quantico, Virginia 22134

Director
National Bureau of Standards
Washington, D.C. 20234
Attn: Mr. B.L. Wilson, EN 219

Dr. M. Gaus
National Science Foundation
Engineering Division
Washington, D.C. 20550

Science & Tech. Division
Library of Congress
Washington, D.C. 20540

Director
Defense Nuclear Agency
Washington, D.C. 20305
Attn: SPSS

Commander Field Command
Defense Nuclear Agency
Sandia Base
Albuquerque, New Mexico 87115

Director Defense Research & Engr
Technical Library
Room 3C-128
The Pentagon
Washington, D.C. 20301

Chief, Airframe & Equipment Branch
FS-120
Office of Flight Standards
Federal Aviation Agency
Washington, D.C. 20553

Chief, Research and Development
Maritime Administration
Washington, D.C. 20235

Deputy Chief, Office of Ship Constr.
Maritime Administration
Washington, D.C. 20235
Attn: Mr. U.L. Russo

Atomic Energy Commission
Div. of Reactor Devel. & Tech.
Germantown, Maryland 20767

Ship Hull Research Committee
National Research Council
National Academy of Sciences
2101 Constitution Avenue
Washington, D.C. 20418
Attn: Mr. A.R. Lytle

Part 2 - Contractors and Other Technical Collaborators

Universities

Dr. J. Tinsley Oden
University of Texas at Austin
345 Eng. Science Bldg.
Austin, Texas 78712

Prof. Julius Miklowitz
California Institute of Technology
Div. of Engineering & Applied Sci.
Pasadena, California 91109

Dr. Harold Liebowitz, Dean
School of Engr. & Applied Science
George Washington University
725 - 23rd St., N.W.
Washington, D.C. 20006

Prof. Eli Sternberg
California Institute of Technology
Div. of Engr. & Applied Sciences
Pasadena, California 91109

Prof. Paul M. Naghdi
University of California
Div. of Applied Mechanics
Etcheverry Hall
Berkeley, California 94720

Professor P.S. Symonds
Brown University
Division of Engineering
Providence, R.I. 02912

Prof. A.J. Durelli
John F. Dodge Professor
Oakland University
Rochester, Michigan 48063

Prof. R.B. Testa
Columbia University
Dept. of Civil Engineering
S.W. Mudd Bldg.
New York, New York 10027

Prof. H.H. Bleich
Columbia University
Dept. of Civil Engineering
Amsterdam & 120th St.
New York, New York 10027

Prof. F.L. DiMaggio
Columbia University
Dept. of Civil Engineering
616 Mudd Building
New York, New York 10027

Prof. A.M. Freudenthal
George Washington University
School of Engineering & Applied Science
Washington, D.C. 20006

D.C. Evans
University of Utah
Computer Science Division
Salt Lake City, Utah 84112

Prof. Norman Jones
Massachusetts Inst. of Technology
Dept. of Naval Architecture & Marine Engrng
Cambridge, Massachusetts 02139

Asst. to Secretary Defense
Atomic Energy-Att. E. Cotter
Washington, D.C. 20301

Dr. W.R. Hodgson
Wayne State University
School of Medicine
Detroit, Michigan 48202

Universities cont.

Dean B.A. Boley
Northwestern University
Technological Institute
2145 Sheridan Road
Evanston, Illinois 60201

Prof. P.G. Hodge, Jr.
University of Minnesota
Dept. of Aerospace Engng & Mech.
Minneapolis, Minnesota 55455

Dr. D.C. Drucker
University of Illinois
Dean of Engineering
Urbana, Illinois 61801

Prof. N.M. Newmark
University of Illinois
Dept. of Civil Engineering
Urbana, Illinois 61801

Prof. E. Reissner
University of California, San Diego
Dept. of Applied Mechanics
La Jolla, California 92037

Prof. William A. Nash
University of Massachusetts
Dept. of Mechanics & Aerospace Eng.
Amherst, Massachusetts 01002

Library (Code 0384)
U.S. Naval Postgraduate School
Monterey, California 93940

Prof. Arnold Allentuch
Newark College of Engineering
Dept. of Mechanical Engineering
323 High Street
Newark, New Jersey 07102

Dr. George Herrmann
Stanford University
Dept. of Applied Mechanics
Stanford, California 94305

Prof. J.D. Achenbach
Northwestern University
Dept. of Civil Engineering
Evanston, Illinois 60201

Director, Applied Research Lab.
Pennsylvania State University
P.O. Box 30
State College, Pennsylvania 16801

Prof. Eugen J. Skudrzyk
Pennsylvania State University
Applied Research Laboratory
Dept. of Physics - P.O. Box 30
State College, Pennsylvania 16801

Prof. J. Kempner
Polytechnic Institute of Brooklyn
Dept. of Aero. Engrg & Applied Mech.
333 Jay Street
Brooklyn, N.Y. 11201

Prof. J. Klosner
Polytechnic Institute of Brooklyn
Dept. of Aerospace & Appl. Mech.
333 Jay Street
Brooklyn, N.Y. 11201

Prof. R.A. Schapery
Texas A&M University
Dept. of Civil Engineering
College Station, Texas 77840

Prof. W.D. Pilkey
University of Virginia
Dept. of Aerospace Engineering
Charlottesville, Virginia 22903

Dr. H.G. Schaeffer
University of Maryland
Aerospace Engineering Dept.
College Park, Maryland 20742

Prof. K.D. Willmert
Clarkson College of Technology
Dept. of Mechanical Engineering
Potsdam, N.Y. 13676

Dr. J.A. Stricklin
Texas A&M University
Aerospace Engineering Dept.
College Station, Texas 77843

Dr. L.A. Schmit
University of California, LA
School of Engineering & Applied Sci.
Los Angeles, California 90024

Dr. H.A. Kamel
The University of Arizona
Aerospace & Mech. Engineering Dept.
Tucson, Arizona 85721

Dr. B.S. Berger
University of Maryland
Dept. of Mechanical Engineering
College Park, Maryland 20742

Prof. G.R. Irwin
Dept. of Mechanical Engng.
University of Maryland
College Park, Maryland 20742

Dr. S.J. Fenves
Carnegie-Mellon University
Dept. of Civil Engineering
Schenley Park
Pittsburgh, Pennsylvania 15213

Dr. Ronald L. Huston
Dept. of Engineering Analysis
Mail Box 112
University of Cincinnati
Cincinnati, Ohio 45221

Prof. George Sih
Dept. of Mechanics
Lehigh University
Bethlehem, Pennsylvania 18015

Prof. A.S. Kobayashi
University of Washington
Dept. of Mechanical Engineering
Seattle, Washington 98105

Librarian
Webb Institute of Naval Architecture
Crescent Beach Road, Glen Cove
Long Island, New York 11542

Prof. Daniel Frederick
Virginia Polytechnic Institute
Dept. of Engineering Mechanics
Blacksburg, Virginia 24061

Prof. A.C. Eringen
Dept. of Aerospace & Mech. Sciences
Princeton University
Princeton, New Jersey 08540

Dr. S.L. Koh
School of Aero., Astro. & Eng. Sc.
Purdue University
Lafayette, Indiana 47907

Prof. E.H. Lee
Div. of Engrg. Mechanics
Stanford University
Stanford, California 94305

Prof. R.D. Mindlin
Dept. of Civil Engrg
Columbia University
S.W. Mudd Building
New York, N.Y. 10027

Prof. S.B. Dong
University of California
Dept. of Mechanics
Los Angeles, California 90024

Prof. Burt Paul
University of Pennsylvania
Towne School of Civil & Mech Engr
Rm. 113 - Towne Building
220 S. 33rd Street
Philadelphia, Pennsylvania 19104

Prof. J.W. Liu
Dept. of Chemical Engr. & Metal.
Syracuse University
Syracuse, N.Y. 13210

Prof. S. Bodner
Technion R&D Foundation
Haifa, Israel

Prof. R.J.H. Bollard
Chairman, Aeronautical Engr. Dept.
207 Guggenheim Hall
University of Washington
Seattle, Washington 98105

Prof. G.S. Heller
Division of Engineering
Brown University
Providence, Rhode Island 02912

Prof. Werner Goldsmith
Dept. of Mechanical Engineering
Div. of Applied Mechanics
University of California
Berkeley, California 94720

Prof. J.R. Rice
Division of Engineering
Brown University
Providence, R.I. 02912

Prof. R.S. Rivlin
Center for the Application of
Mathematics
Lehigh University
Bethlehem, Pennsylvania 18015

Bell Telephone Labs Inc.
505 King Avenue -Tech. Lib.
Columbus, OH 43201

Dr. Francis Cozzarelli
Div. of Interdisciplinary
Studies & Research
School of Engineering
State University of New York
Buffalo, N.Y. 14214

Industry and Research Institutes

Library Services Dept.
Report Section Bldg. 14-14
Argonne National Laboratory
9700 S. Cass Avenue
Argonne, Illinois 60440

Dr. M.C. Junger
Cambridge Acoustical Associates
129 Mount Auburn St.
Cambridge, Massachusetts 02138

Dr. L.H. Chen
General Dynamics Corporation
Electric Boat Division
Groton, Connecticut 06340

Dr. J.E. Greenspon
J.G. Engineering Research Assoc.
3831 Menlo Drive
Baltimore, Maryland 21215

Dr. S. Batdorf
The Aerospace Corp.
P.O. Box 92957
Los Angeles, California 90009

Dr. K.C. Park
Lockheed Palo Alto Research Lab.
Dept. 5233, Bldg. 205
3251 Hanover St.
Palo Alto, CA 94304

Library
Newport News Shipbuilding & Dry
Dock Company
Newport News, Virginia 23607

Dr. W.F. Bozich
McDonnell Douglas Corporation
5301 Bolsa Avenue
Huntington Beach, CA 92647

Dr. H.N. Abramson
Southwest Research Institute
Technical Vice President
Mechanical Sciences
P.O. Drawer 28510
San Antonio, Texas 78284

Dr. R.C. DeHart
Southwest Research Institute
Dept. of Structural Research
P.O. Drawer 28510
San Antonio, Texas 78284

Dr. M.L. Baron
Weidlinger Associates, Consulting
Engineers
110 East 59th Street
New York, N.Y. 10022

Dr. W.A. Von Riesmann
Sandia Laboratories
Sandia Base
Albuquerque, New Mexico 87115

Dr. T.L. Geers
Lockheed Missiles & Space Co.
Palo Alto Research Laboratory
3251 Hanover Street
Palo Alto, California 94304

Dr. J.L. Tocher
Boeing Computer Services, Inc.
P.O Box 24346
Seattle, Washington 98124

Mr. William Caywood
Code BBE, Applied Physics Laboratory
8621 Georgia Avenue
Silver Spring, Maryland 20034

Mr. P.C. Durup
Lockheed-California Company
Aeromechanics Dept., 74-43
Burbank, California 91503

Assistant Chief for Technology
Office of Naval Research, Code 200
Arlington, Virginia 22217

Los Alamos Scientific Lab
P.O. Box 1663 - Tech Labs
Los Alamos, NM 87544

Boeing Company
Attn. Aerospace Lab
P.O. Box 3707
Seattle, WA 98124

IIT Research Institute
10 West 35th Street
Chicago, ILL 60616

Unclassified

SECURITY CLASSIFICATION OF THIS PAGE (When Data Entered)

(14) **REPORT DOCUMENTATION PAGE**

READ INSTRUCTIONS BEFORE COMPLETING FORM

1. REPORT NUMBER: ONR-UC-ES-08177-4-ONR (9) Final, technical, rept. 1 Jan 75-30 Sep 76

2. GOVT ACCESSION NO.

3. RECIPIENT'S CATALOG NUMBER

(6) 4. TITLE (and Subtitle): Multi-Rigid-Body System Dynamics with Applications to Human-Body Models and Finite-Segment Cable Models

5. TYPE OF REPORT & PERIOD COVERED: Technical 1/1/75-9/30/76 Final

6. PERFORMING ORG. REPORT NUMBER

(10) 7. AUTHOR(s): Ronald L. Huston, Chris E. Passerello

(15) 8. CONTRACT OR GRANT NUMBER(s): N0014-75-C-1164

9. PERFORMING ORGANIZATION NAME AND ADDRESS: University of Cincinnati, Cincinnati, Ohio 45221

10. PROGRAM ELEMENT, PROJECT, TASK AREA & WORK UNIT NUMBERS: 122303

(11) 11. CONTROLLING OFFICE NAME AND ADDRESS: Office of Naval Research Resident Representation, Purdue University, Rm 84 Graduate House, Lafayette, Indiana 47907

12. REPORT DATE: 8/1/77 (1 Aug 77)

13. NUMBER OF PAGES

14. MONITORING AGENCY NAME & ADDRESS (if different from Controlling Office): Office of Naval Research, Structural Mechanics, Department of the Navy, Arlington, Va. 22217

(12) 15. SECURITY CLASS. (of this report): Unclassified (66 p.)

15a. DECLASSIFICATION/DOWNGRADING SCHEDULE

16. DISTRIBUTION STATEMENT (of this Report)

Distribution of this report is unlimited

17. DISTRIBUTION STATEMENT (of the abstract entered in Block 20, if different from Report)

18. SUPPLEMENTARY NOTES

19. KEY WORDS (Continue on reverse side if necessary and identify by block number)

Dynamic System Modelling, Human Body Dynamics, Crash Victim Simulation, Cable Modelling, Finite-Segment Modelling, Biodynamic Modelling, Impact Simulation

20. ABSTRACT (Continue on reverse side if necessary and identify by block number)

A computer-oriented method for obtaining dynamical equations of motion for large mechanical systems or "chain systems" is presented. A chain system is defined as an arbitrarily assembled set of rigid bodies such that adjoining bodies have at least one common point and such that closed loops are not formed. The equations of motion are developed through the use of Lagrange's form of d'Alembert's principle.

over

DD FORM 1 JAN 73 1473 EDITION OF 1 NOV 65 IS OBSOLETE S/N 0102-014-6601 |

SECURITY CLASSIFICATION OF THIS PAGE (When Data Entered)

410649

20.

The method is illustrated and applied with human-body models and finite-segment cable models. The human-body models are configured to simulate a crash-victim. Results with several applied deceleration profiles agree very well with available experimental data. The cable model is configured to simulate an off-shore oil rig or ship's crane with a partially submerged towing cable.